Comparison of Finite Element Method and Modal Analysis of Violin Top Plate

Ye Lu

Music Technology Area, Department of Music Research
Schulich School of Music
McGill University
Montreal, Canada

June 2013

A thesis submitted to McGill University in partial fulfillment of the requirements for the degree of Master of Arts in Music Technology.

© 2013 Ye Lu

2013/06/04

Abstract

This thesis presents a study of the vibrational behaviour of the violin top plate and explores the possibility of using composite materials as a substitute for traditional wood in making top plates. Numerical simulations and experimental tests are compared to validate the results. The two most popular methods for numerical and experimental vibrational analysis, the Finite Element Method (FEM) and Experimental Modal Analysis are used, respectively.

The vibrational behaviour of a spruce top plate is first studied by the two methods. The results show high coherence. Then the same modeling and testing techniques are applied on two composite plates. Results show that the vibrational behaviour of composite plates differs significantly from traditional wooden plates. Thus, suggestions for further improvement of the composite top plates are given.

Sommaire

Cette thése propose une étude sur le comportement vibratoire de la table d'harmonie du violon et explore la possibilité d'utiliser des matériaux composites comme un substitut pour le bois traditionnel dans la fabrication des tables d'harmonies. Des simulations numériques ét des tests exprimentaux sont comparés pour valider les résultats. Les deux méthodes les plus populaires pour l'analyse vibratoire numérique et expérimentale, la méthode des éléments finis (FEM) et l'analyse modale exprimentale sont utilisés, respectivement.

Le comportement vibratoire d'une table d'harmonie en épicéa est d'abord étudiée par les deux méthodes. Les résultats montrent une cohérence forte. Puis la modélisation et même des techniques de test sont appliqués sur deux plaques composites. Les résultats montrent que le comportement vibratoire de table d'harmonie composites diffère sensiblement de plaques traditionnels en bois. Ainsi, des suggestions d'amélioration des tables d'harmonie composites du dessus sont donnés.

Acknowledgments

I would like to gratefully thank Prof. Gary Scavone and Prof. Larry Lessard for their supervision, guidance, and expertise during this work. I would like especially, to thank Gary for providing the various equipment to ensure my experimental test worked smoothly and for spending considerable amount of time on all aspects of my thesis. Also I would like to show my great appreciation to Larry for providing me the very helpful violin top plate prototypes and their very detailed manufacturing data. Many thanks to the luthier Peter Purich for offering the spruce plate and the Chladni pattern photos

I would like to extend my appreciation to the students, faculty and staff of the Music Technology Area at McGill University for their advice, insight and friendship. In particular, I would like to thank the members of the Computational Acoustic Modeling Laboratory (CAML) for providing me a great environment to pursue my research work. I would also take this opportunity to acknowledge Hossein Mansour at CAML for all the meaningful discussions and for his valued assistance. Many thanks to Darryl Cameron and Harold Kilianski for providing necessary equipment and the technical support during my research work. A special thanks to my girlfriend Jenny Liu for kindly providing the proof reading. Finally, the greatest thanks go to my parents in China, for their financial and moral support in my most difficult times.

Contents

1 Introduction **1**
1.1 Motivation 1
1.2 Project Overview 2
1.3 Thesis Overview 3
1.4 Contributions 4

2 Background **5**
2.1 Violin Acoustics 5
2.1.1 The Strings 5
2.1.2 The Bridge 7
2.1.3 The Bass Bar and Soundpost 8
2.1.4 The Soundbox 9
2.2 The Finite Element Method 10
2.2.1 Procedures of the Finite Element Method 10
2.2.2 Node, Element and Shape Function 11
2.2.3 Equation of Motion 13
2.3 Experimental Modal Analysis 17
2.3.1 Mobility Measurement 18
2.3.2 Excitation 19
2.3.3 Coherence Function 20
2.3.4 Windows 21
2.4 Composite Music Instruments 22

3 FEM and Modal Analysis Set-up **25**
3.1 Numerical Model of a Spruce Top Plate 25

3.1.1 CAD Model of a Top Plate . . . 26
3.1.2 Pre-Processing . . . 29
3.1.3 Normal Mode Extraction . . . 33
3.2 Modal Analysis Set-up . . . 34
3.2.1 Experiment Set-up . . . 35
3.2.2 The Choice of the Hammer . . . 37
3.2.3 Accelerometer . . . 40
3.2.4 Selection of the Points . . . 40
3.2.5 Data Acquisition . . . 42
3.2.6 Data Analysis . . . 43
3.2.7 Modal Information Detection . . . 44

4 Comparison of FEM and Modal Analysis Results 49
4.1 FEM Results of the Spruce Plate . . . 49
4.2 Modal Analysis Results of the Spruce Plate . . . 51
4.3 Carbon Fibre Top Plate . . . 52
4.3.1 Choice of the Material . . . 55
4.4 Numerical Simulation of the Composite Top Plates . . . 56
4.5 Modal Analysis of the Composite Top Plates . . . 64

5 Discussion 70
5.1 FEM Results of the Spruce Plate . . . 70
5.2 Comparison of the FEM Results to the Modal Analysis Results of the Spruce Plate . . . 73
5.3 Vibration and Damping of the Composite Plate #1 . . . 74
5.4 Vibration and Damping of the Composite Plate #2 . . . 76
5.5 Comparison of the FRFs by the FEM and the Modal Analysis . . . 78
5.6 FEM Experiments on Different Layer Combinations . . . 79

6 Conclusions and Future Work 85
6.1 Conclusions . . . 85
6.2 Future Work . . . 86

References 87

List of Figures

2.1 Structure of a violin [1] 6
2.2 The bridge of a violin [2] 8
2.3 A single harmonic oscillator 14
2.4 A violin top plate 14
2.5 A discretized violin top plate 15
2.6 A coherence function in the test 21

3.1 The spruce top plate 26
3.2 A set of selected points for defining the arch height 28
3.3 CAD drawing of the spruce top plate 29
3.4 Meshing of the spruce top plate 30
3.5 Collectors of the top plate 31
3.6 Typical setup for a roving impact hammer test on a cantilever beam [3] . . 35
3.7 The experiment set-up 36
3.8 The pendulum system 37
3.9 Impact Hammer Model 086E80 38
3.10 Accelerometer Model 352C23/NC 40
3.11 Selected hitting points 42
3.12 Marked points on the spruce plate 43
3.13 Experimental Setup #2 45
3.14 The FRF and the coherence function of point 2 46
3.15 Overlapped FRFs 46
3.16 Plate mode shape for mode 2 [3] 47

4.1 Mode 1 of the spruce plate by the FEM and the Chladni Method 50

4.2 Mode 2 of the spruce plate by the FEM and the Chladni Method 50
4.3 Mode 5 of the spruce plate by the FEM and the Chladni Method 51
4.4 Comparison of Mode 1 of the spruce plate by the FEM and the Modal Analysis 51
4.5 Comparison of Mode 2 of the spruce plate by the FEM and the Modal Analysis 52
4.6 Comparison of Mode 3 of the spruce plate by the FEM and the Modal Analysis 52
4.7 Comparison of Mode 4 of the spruce plate by the FEM and the Modal Analysis 53
4.8 Comparison of Mode 5 of the spruce plate by the FEM and the Modal Analysis 53
4.9 Comparison of Mode 6 of the spruce plate by the FEM and the Modal Analysis 54
4.10 Components of the second composite plate 55
4.11 Stage 1 of making a composite plate (layers cut and put in mould) 56
4.12 Stage 2 of making a composite plate (air extracted) 56
4.13 Stage 3 of making a composite plate (vacuum attached) 57
4.14 Stage 4 of making a composite plate (after curing) 57
4.15 Stage 1 of making the urethane ring 57
4.16 Stage 2 of making the urethane ring 57
4.17 Components of the composite plate #1 58
4.18 Comparison of Mode 1 of the composite plate #1 by the FEM and the Modal Analysis 60
4.19 Comparison of Mode 2 of the composite plate #1 by the FEM and the Modal Analysis 61
4.20 Comparison of Mode 3 of the composite plate #1 by the FEM and the Modal Analysis 61
4.21 Comparison of Mode 4 of the composite plate #1 by the FEM and the Modal Analysis 62
4.22 Comparison of Mode 5 of the composite plate #1 by the FEM and the Modal Analysis 62
4.23 Comparison of Mode 6 of the composite plate #1 by the FEM and the Modal Analysis 63
4.24 Components of the composite plate#2 63
4.25 Comparison of Mode 1 of the composite plate #2 by the FEM and the Modal Analysis 65
4.26 Comparison of Mode 2 of the composite plate #2 by the FEM and the Modal Analysis 65

4.27 Comparison of Mode 3 of the composite plate #2 by the FEM and the Modal Analysis 66
4.28 Comparison of Mode 4 of the composite plate #2 by the FEM and the Modal Analysis 66
4.29 Comparison of Mode 5 of the composite plate #2 by the FEM and the Modal Analysis 67
4.30 Comparison of Mode 6 of the composite plate #2 by the FEM and the Modal Analysis 67

5.1 The first six modes of the spruce plate by the FEM (Bretos) [4] 71
5.2 The first six modes of the spruce plate by the FEM (Molin) [5] 72
5.3 The first six modes of the spruce plate by the FEM 72
5.4 FRF of the spruce plate by the FEM 80
5.5 FRF of the spruce plate by the Modal Analysis 80
5.6 FRF of the composite plate #1 by the FEM 81
5.7 FRF of the composite plate #1 by the Modal Analysis 81
5.8 FRF of the composite plate #2 by the FEM 82
5.9 FRF of the composite plate #2 by the Modal Analysis 82
5.10 Layup 1 83
5.11 Layup 2 83
5.12 Layup 3 83
5.13 Layup 4 84

List of Tables

3.1 Width and length of the plate 27
3.2 A set of selected points for defining the arch height 27
3.3 Arch height at a set of selected points 32
3.4 Elastic parameters and density of the spruce 32
3.5 Specifications of the hammer 39
3.6 Specifications of the accelerometer 41

4.1 Natural frequencies of the spruce top plate by FEM 49
4.2 Natural frequencies of the spruce top plate by modal analysis 54
4.3 Material properties of spruce, balsa and MTM45-1 59
4.4 Natural frequencies of the composite plate #1 by FEM 60
4.5 Material properties of Newport301 64
4.6 Natural frequencies of the composite plate #2 by the FEM 64
4.7 Natural frequencies of the composite plate #1 by the modal analysis . . . 68
4.8 Natural frequencies of the composite plate #2 by the modal analysis . . . 69

5.1 Comparison of the natural frequencies by the FEM of the spruce plate with previous research 73
5.2 Comparison of the natural frequencies by the FEM and the modal analysis of the spruce plate 74
5.3 Comparison of the natural frequencies by the FEM and the modal analysis of the spruce plate and the composite plate #1 75
5.4 Comparison of the damping ratios of the spruce and the composite plates . 76
5.5 Comparison of the natural frequencies by the FEM and the modal analysis of the spruce plate and the composite plate #2 77

5.6 Comparison of the natural frequencies by the FEM of different composite plate layups 84

List of Acronyms

FEM	Finite Element Method
DOF	Degree of Freedom
MDOF	Multi-Degree-Of-Freedom
CAD	Computer-Aided-Design
FRF	Frequency Response Function

Chapter 1

Introduction

1.1 Motivation

The study of a violin's vibrational and acoustical properties has been popular over the last several decades. A typical violin is made up of several parts: a top plate, back plate, ribs, bass bar, sound post, neck, scroll, etc. The design of the top plate has a strong influence on the timbral quality of a violin [6]. It is not easy to make a good top plate because the luthier must not only choose the most suitable wood (light, stiff, low friction, a specific relation between the transversal and the longitudinal stiffness, etc.), but must also carefully define the arching shape and thickness distribution [7].

In my thesis, both numerical and experimental methods were used to test and compare the vibrational behavior of violin top plates. The research considered top plates made of both spruce and composite materials. The analysis of the properties of new materials (such as carbon fibre) were conducted under the partial supervision of Professor Larry Lessard in the Mechanical Engineering Department. By analyzing the vibrational patterns of violin top plates using these methods, an insight was gained into the acoustical behaviour of the plate. The comparison of the numerical simulation and experimental tests was used to validate the results. This research might potentially allow for the optimized design of violin top plates and be useful as a theoretical basis for manufacturing consistently good violins.

Research on violins is not a new topic. Indeed, one might argue that luthiers have been conducting empirical research on violins for well over 400 years, with results from 300 years ago still considered by many to epitomize the best available specimens [8]. Hutchins

was the first one to point out the importance of the plates on the tuning of the violin [6, 9]. Over the past few decades, several numerical and experimental techniques have been applied to the analysis of violin top plates. Two of them, the Finite Element Method (FEM) [10, 5, 11, 4, 12] and the Modal Analysis [13, 14, 15, 16, 17], are very popular because they provide good results that can be compared to one another. Several researchers have looked at different aspects of the optimization of the top plate by using these two methods. Loen has studied the graduation patterns and thickness distributions of many classic Cremonese violins [18]. Tinnsten et al. have used the simulated annealing method to compensate material parameters with thickness variation [19]. Yu et al. have studied nodal line optimization to maximize the vibration of the top plate [20]. The quest for new materials to replace wood in the top plates has also been a hot topic during these years [21, 22]. Due to the development of advanced manufacturing technologies, composite materials of superior performance can be achieved, by choosing and adjusting their material properties carefully.

1.2 Project Overview

The goal of my research project was to study the vibrational behaviour of the violin top plate. Both numerical and experimental methods were used and compared with each other to validate the numerical model. The normal modes (resonances) of vibration and their frequencies were determined by both methods. Different geometry and material properties were also tested to see how they influence the mode sensitivities.

The first step of my project was to make a geometrical model of the top plate. There are various commercial Computer Aided Design (CAD) software packages available including AutoCAD, SolidWorks, UniGraphics, CATIA, and Pro/Engineer. SolidWorks was selected because it has powerful surface generating functions and it is easier to change parameters directly in this software. The dimensions of the plate and the arch height were varied around known values from violins considered to be of high quality.

After the mesh (a discretized geometry which is used for calculation) is made, it will be used for the numerical simulation. The Finite Element Method (FEM), which is a numerical technique particularly good at solving complex structural problems, were used. The idea was to discretize the top plate structure into regions, each of which has many smaller elements called nodes (intersections of mesh elements). Properties of the material (wood or

carbon fibre) were defined in terms of elasticity and density and then the theoretical vibrational behaviour of the structure was solved through matrix manipulations. This allowed the primary eigenfrequencies of a structure to be determined, as well as the visualization of the mode shapes. The commercial software package ANSYS was used for the calculations, together with the pre-processing software HyperMesh to mesh the structure and define the loads and boundary conditions. Different structural parameters (thickness, arch height, bass bar) and materials (spruce and carbon fiber) were simulated. Subsequently, a Modal Analysis of both spruce and composite top plates was performed. The process involved hanging each plate (to achieve a free-free boundary condition) and then recording the response of the plates (using a miniature accelerometer) to a sequence of "taps" at various locations (using an instrumented miniature force hammer). Both the input and output response data was input into a Modal Analysis software, ME'Scope, that can extract eigenfrequencies and visualize the modal shapes. The next step was to compare the Finite Element results with Modal Analysis results. The parameters of the FEM were carefully adjusted in order to get satisfactory results.

1.3 Thesis Overview

Chapter 2 will provide an introduction to violin acoustics, the idea of how to implement FEM and Modal Analysis, and the usage of composite materials on the musical instrument. This information will give the reader a clear idea about how things work in the later chapters.

Chapter 3 will deal with the numerical simulation and the experimental test set-up of the spruce plate. Comparisons with previous research will be provided, though a detailed analysis of the results will be left for subsequent chapters.

Chapter 4 will discuss the numerical simulation and the experimental test results on both the spruce and the composite plates. The manufacturing process of the composite plates will also be discussed.

Chapter 5 will include an analysis of the data from the previous two chapters. Discussions will focus on how the geometry and the material property variations influence the vibrational behaviour of the plate.

Chapter 6 will summarize the results and conclusions obtained in general. A few potential research goals for the future will also be suggested.

1.4 Contributions

After carefully adjusting the parameters of the FEM, it can be used as a tool for the design optimization of violin top plates. Instead of manually adjusting the arch height and thickness of the plate to experiment with variations of geometric features, a numerical simulation can be performed to estimate the resulting effect. The comparison of numerical and experimental results can also provide some information about how a plate made of new materials (such as carbon fiber) behaves in comparison to the traditional wooden plate. Compared to wood, composite materials have more flexible properties and are easier to manufacture. The results of this thesis might push forward the application of composite materials in the music instrument industry.

Chapter 2

Background

2.1 Violin Acoustics

The violin is one of the most representative instruments in the string family. Over the past three hundred years, both musicians and scientists have made great efforts to try to understand the complicated vibration mechanisms behind its mellifluous sound. Their research on violin acoustics has focused on different aspects, including the material properties of the wood, the body vibration modes, the air cavity modes coupled with the body, the radiation from the f-holes and so on.

A typical violin can be divided into several parts: a bow which provides excitation to the strings; several strings which are attached at the scroll and the tailpiece with high tensions; a bridge which supports the strings and transmits the vibration energy to the body; a bass bar and a soundpost which provide support to the top plate and help to better transmit the vibrations from the top plate to the soundbox; and a soundbox which serves as a resonator. There are also several acoustically less important components, such as the neck and the chinrest which the musician holds to make the instrument stable when playing. A disassembled violin is shown in Fig. 2.1.

2.1.1 The Strings

The strings receive energy from the bow and are forced to vibrate. They are stretched and fixed at both the scroll and the tailpiece, so that standing waves are generated when they vibrate. The pitch of a fixed string is determined by its length, diameter, density and

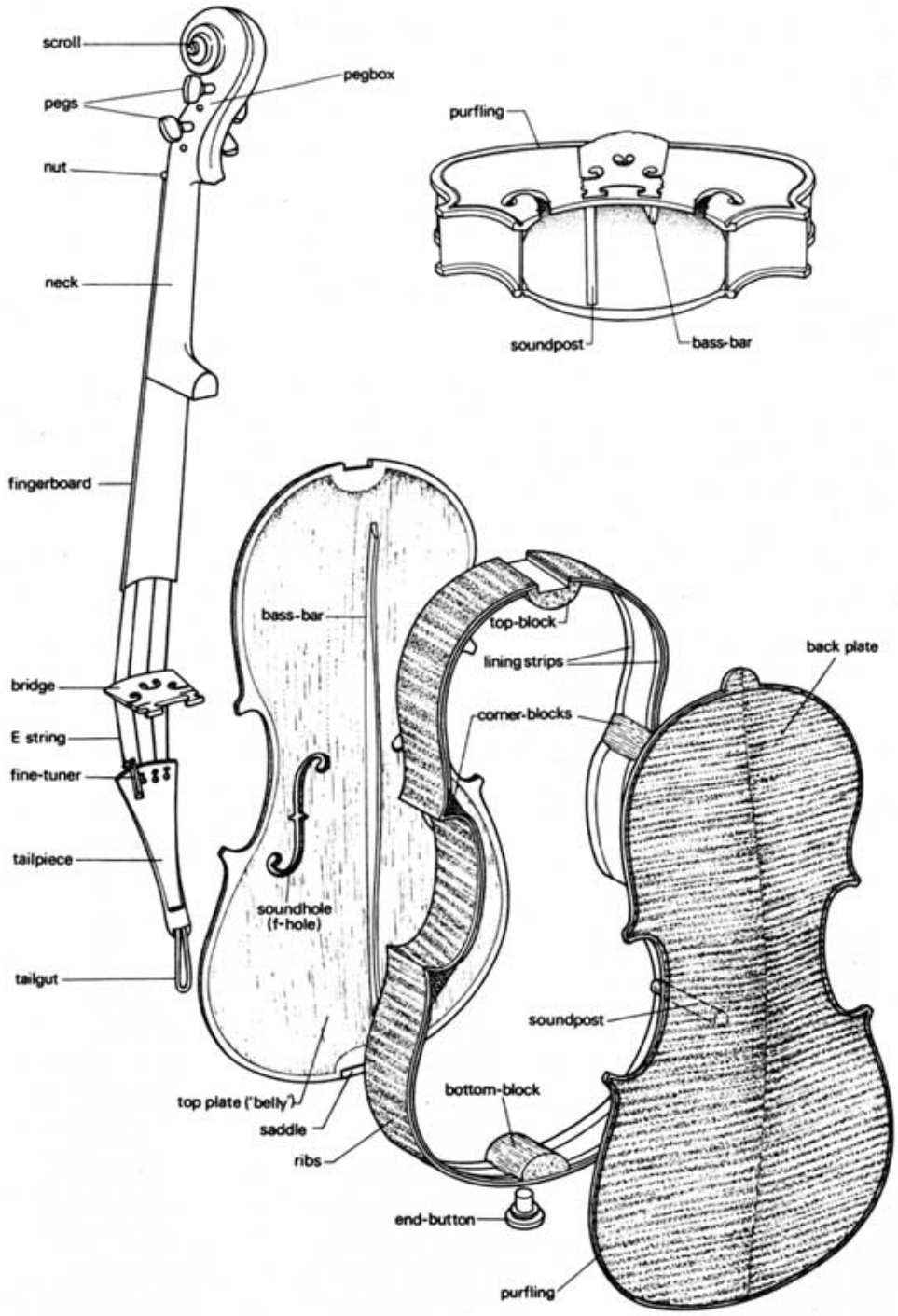

Fig. 2.1 Structure of a violin [1]

torsion. Several types of materials are most often used for making violin strings. Gut core strings have the longest history. They can produce warm and rich sounds. Back in the sixteenth century, the gut strings were made purely of sheep gut, while today's gut strings often have only the gut core covered by copper or silver. Steel core strings are another popular type of strings nowadays. They usually have more overtones compared to gut strings because they have less internal damping. Due to the stable behavior of steel, these strings are less sensitive to the environment, and can last longer. Synthetic core strings use new materials and became available in the 1970s. They are basically made of nylon and composite materials, which have an even warmer timbre than gut strings, as well as a longer lifetime than steel strings.

When a string vibrates, there will be a dominant fundamental frequency and several overtones which are harmonic to that frequency. For instance, if a violinist plays an A4 note, the fundamental frequency will be 440 Hz, and there will also be harmonic overtones which have frequencies of 880 Hz, 1320 Hz, 1760 Hz, 2200 Hz and so on. The overtones will drop off in amplitude with frequency but some of the lower frequency components can be as strong or nearly as strong as the fundamental. These overtones play an important role in constructing the timbre of the note.

Strings are changed quite often during the whole life of a violin. Strings from a certain brand may sound fantastic on one violin but not as good on another. A violinist might need to spend great effort finding a type of string which can produce the best sounds on his or her violin.

2.1.2 The Bridge

The bridge, as shown in Fig. 2.2, transfers the vibration energy of the strings to the violin body via two feet which rest on the top plate, parallel to the notches of the f-holes. One foot is right above the bass bar and another is very close to the soundpost. The bridge works as a filter for different wavelengths of sound. Bridges are usually made of maple, which is also very often used to make the back plate. This wood is stiffer than spruce and balsa and is good for withstanding the pressure applied by the strings. The two feet of the bridge are carved to fit the curvature of the top plate. At the intersection, the bridge is purely clamped by the strings and the top plate without glue. The four notches on the top of the bridge and the two feet make it stand stable.

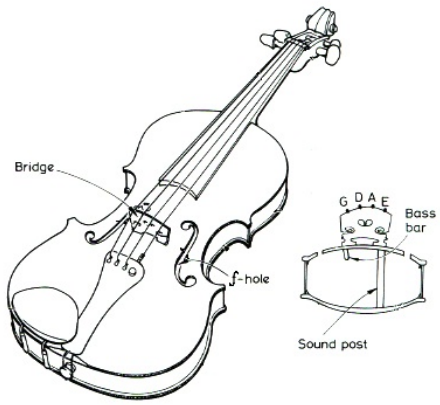

Fig. 2.2 The bridge of a violin [2]

The bridge is not symmetric in either direction. From the front view, the notch of the G string is a little bit lower than the notch of the E string, which makes it easier for the player to control the strings. From the side view, one side is flat, another is slightly tapered. The flat side faces the scroll and the tapered side faces the tailpiece, which makes the bridge stand more stable on the top plate.

Since the bridge stands at the most sensitive position of a violin, even very tiny changes in its shape or position can make perceptible differences to the timbre. Previous research showed that modifications of its shape, density and the stiffness, as well as the position of the two feet, will cause shifts of the natural frequencies of the violin body [23, 24].

2.1.3 The Bass Bar and Soundpost

The bass bar is glued rigidly to the top plate and it is positioned right below the G-string foot of the bridge. The bass bar serves as a support for the top plate against the high bending forces applied by the strings. Another function of the bass bar is to help spread the vibration energy from the string to the upper bout and lower bout of the top plate.

The presence of the bass bar shifts the natural frequencies of the top plate. It also makes the mode shapes asymmetric and changes the nodal line positions of certain modes. It is found that the bass bar can be carefully tuned to match the stiffness of a top plate. Thus when it is glued to that plate, the amplitude of the tap tone and the damping can be adjusted to an optimum value [25].

The sound post also plays an important role in the violin acoustics. It is proven that one role of the soundpost is to introduce some asymmetry to the body vibration. On some instruments, one foot of the bridge is simply elongated to replicate the sound post, thus providing asymmetry [26].

Another function of the soundpost is to help better transfer the vibration energy from the top plate to the back plate. Researchers also showed that by moving the sound post inside the body, a phase difference can be made for the top plate and the back plate when they are vibrating [13].

2.1.4 The Soundbox

The soundbox consists of the top plate, back plate (also called "the belly"), and the ribs. The plates are carefully tuned before being assembled. Before assemblage, luthiers use various means to get the best sound quality of the plates. The "tap tone" method is one of the easiest to try, in which luthiers tap on the plate in order to determine whether it has a similar sound compared to plates previously known to be "good". In order to modify the sound quality, tiny adjustments of the thickness and the geometry are made to the plates. Nowadays, many luthiers also use the Chaldni method to more accurately detect the modes of the plate [6]. The idea is to put some sand on the plate and use a shaker to excite the structure over a range of frequencies. When the driving frequency fits the natural frequency of the plate, the mode at that frequency is excited, and the sand will collect near the node lines of that mode. By applying this method, luthiers can easily determine the frequencies of the normal modes as well as the mode shapes. This method gives a clearer idea about the quality of the top plate than the traditional "tap tone" method because the latter usually requires excellent absolute pitch and aural memory.

Regarding the tonal quality, C.M. Hutchins suggested certain relationships for mode frequencies and amplitudes. She pointed out that the "ring mode" (whose mode shape is like a ring), which is usually the fifth normal mode of the top plate, should be excited as much as possible. Also, she suggested that an acoustically good violin plate should have octave relationships for its first, second, and fifth modes [6] (this point is doubted by some other researchers). However, it is still unclear whether these suggestions are actually agreed upon by luthiers or researchers.

The top and back plates are connected with ribs by glue. The ribs are very carefully

shaped by heat. The ribs are made of maple and they are usually very thin (about 1mm).

The body of the violin serves as a resonator. When the string energy is transferred to the top plate, the body helps convert the mechanical vibrations to acoustic vibrations, radiating them into the air. The air modes inside the body couple with the body modes, which makes the vibration behavior and the mode shapes more complicated.

Much previous research has focused on modal analysis of the whole body [13, 27, 28]. Most of these chose the excitation position at the bridge since this is the position where energy gets transferred from the strings. Numerical methods (such as the Finite Element Method) are also used to predict the vibrational behaviour of the violin body [29]. However, the condition is more complicated here than analyzing the top plate since the soundpost and the ribs are not rigidly glued to the top and back plate.

2.2 The Finite Element Method

The Finite Element Method (FEM) is a powerful numerical method for solving complex differential equations. The idea of FEM is to discretize a complex structure into relatively simple substructures called "elements". Then the elements are connected in a certain manner, appropriate boundary and load conditions applied, and approximate solutions to the problem determined. Since the violin top plate has a relatively complex geometry, it is hard to describe it with a set of differential equations and analytically solve them. In such a case, the Finite Element Method is particularly useful for calculating the natural frequencies and the mode shapes of the violin top plate.

2.2.1 Procedures of the Finite Element Method

The execution of a typical commercial Finite Element Method software can usually be divided into three stages: Pre-Processing, Processing and Post-Processing.

The Pre-Processing stage includes defining the element types, meshing the system, assigning material properties to each element and setting the boundary conditions and the loads. The understanding of the physical principles behind the problem is always more important than the modeling technique itself. If the boundary conditions are incorrect, or if the element type is not properly chosen, the results could be erroneous.

Many commercial Pre-Processing software systems (such as HyperMesh and Gambit) offer user-friendly interfaces. Usually the user does not have to directly deal with the

sophisticated matrix transformations; he or she would only need to click on the screen to choose the nodes and input all the coefficients.

The Processing stage is more straightforward. The pre-processed model is imported into a solver, and then the solver will assemble the stiffness matrix and calculate all the Degrees of Freedom (DOFs). This process might take several seconds to several days, depending on the number of elements and the computational ability of the computer.

The Post-Processing stage allows visualization of the calculated data. Based on the calculated DOFs, different graphs can be drawn based on the user's preference. For instance, one can choose either the stress or the strain distribution, although the calculated DOFs are in the form of displacements. The visualization of the results provides a very direct idea for structure modifications.

2.2.2 Node, Element and Shape Function

It is mathematically difficult to define a complex structure with a set of prescribed functions and proper boundary conditions. And it is even more difficult to analytically solve a set of functions like this. The FEM is particularly useful in solving complicated differential equations with numerical solutions. The FEM works by approximating the shape of a structure with a finite number of smaller geometrical segments for which analytical functions can be defined and solved. The overall behaviour of the complete structure is then found by solving the functions. The continuous structure can be discretized into a set of "Elements", each containing several "Nodes". Each node will have several DOFs. A DOF can be any physical unit which must be solved in the differential equation, e.g. displacement, velocity, pressure. A node or element can have different types of DOFs. For instance, a 4-node-8-DOF element can have either two translational DOFs or one translational DOF and one rotational DOF on each node.

The shape function is used to interpolate computed values between the nodes. Usually a shape function has the form of a polynomial function. Given a differential equation of the form:

$$\zeta\left(u(x), u(\dot{x}), u(\ddot{x}), x\right) = 0, \tag{2.1}$$

the approximate solution $u(x)$ of the problem can be expressed by truncating n terms of

its Taylor expansion:

$$u(x) \cong a_0 + a_1 x + a_2 x^2 + a_3 x^3 + ...a_n x^n = \sum_{i=0}^{n} a_i x^i. \tag{2.2}$$

This approximate solution can also be represented with a set of DOFs at the nodes:

$$u(x) \cong N_1(x)u_1(x) + N_2(x)u_2(x) + N_3(x)u_3(x) + ...N_n(x)u_n(x) = \sum_{i=1}^{n} N_i(x)u_i(x), \tag{2.3}$$

where N_i is the shape function at node i and $u_i(x)$ is the DOF at node i.

A feature of the shape function is $N_i(x) = 1$ at node i, and $N_i(x) = 0$ at other nodes. In this manner, each shape function can represent the weight of the corresponding node.

Consider a simple 2-node-2-DOF bar element:

For this element, the solution can be expressed as:

$$u(x) \cong a_0 + a_1 x = \sum_{i=1}^{1} a_i x^i, \tag{2.4}$$

where $u(x)$ is the global solution, x is the global variable, and a_0, a_1 are coefficients which can be expressed by x_1 and x_2 (the value of x at the two nodes). The element can be represented in matrix form as:

$$\begin{bmatrix} u_1 \\ u_2 \end{bmatrix} = \begin{bmatrix} 1 & x_1 \\ 1 & x_2 \end{bmatrix} \begin{bmatrix} a_0 \\ a_1 \end{bmatrix}. \tag{2.5}$$

where $u_1 = u(x_1)$ and $u_2 = u(x_2)$.

Solving for a_0 and a_1, we have:

$$\begin{aligned} a_0 &= u_1 - \frac{u_2 - u_1}{x_2 - x_1} x_1 \\ a_1 &= \frac{u_2 - u_1}{x_2 - x_1} \end{aligned} \tag{2.6}$$

The solution $u(x)$ can be represented as:

$$\begin{aligned} u(x) &= \left(u_1 - \frac{u_2 - u_1}{x_2 - x_1} x_1\right) + \left(\frac{u_2 - u_1}{x_2 - x_1}\right) x \\ &= \left(\frac{x_2 - x}{x_2 - x_1}\right) u_1 + \left(\frac{x - x_1}{x_2 - x_1}\right) u_2 \\ &= N_1 u_1 + N_2 u_2 \end{aligned} \tag{2.7}$$

and the shape function N can be represented as:

$$N = \begin{bmatrix} \frac{x_2 - x}{x_2 - x_1} \\ \frac{x - x_1}{x_2 - x_1} \end{bmatrix}, \tag{2.8}$$

where x_1 and x_2 are the coordinates at the two ends of the bar and x could be any point on this element. In this case we have the simplest 2-Node-2-DOF 1D Bar Element. In practical engineering problems, 2D and 3D elements are used very often. In a commercial software, a 2D element can usually have up to 8 nodes and 48 DOF, and a 3D element can usually have up to 27 nodes and 60 DOFs (rotational DOFs of 3D element are often omitted in commercial software). No matter how large the element is, it is always necessary to find an expression for the shape functions and these shape functions are used to calculate the mass and stiffness matrices of the element, as shown in the next chapter.

2.2.3 Equation of Motion

A vibration problem can be described by a general equation of motion, which follows Newton's laws of motion. Let's first consider the equation of motion of a single harmonic oscillator:

$$m\frac{d^2x}{dt^2} + c\frac{dx}{dt} + kx = F, \tag{2.9}$$

where m is the mass of the oscillator, c is the damping coefficient of the oscillator, k is the stiffness of the oscillator and F is the external force. This equation can describe the vibrational behavior of a damped oscillator, as shown in Fig. 2.3:

Most of the vibration problems in real life are far more complicated than simply solving the vibration of an oscillator. Usually a complex structure (such as violin top plate) has more than one natural frequency. If the problem is assumed linear, the structure can be considered as the sum of a bunch of harmonic oscillators, and the structure will have

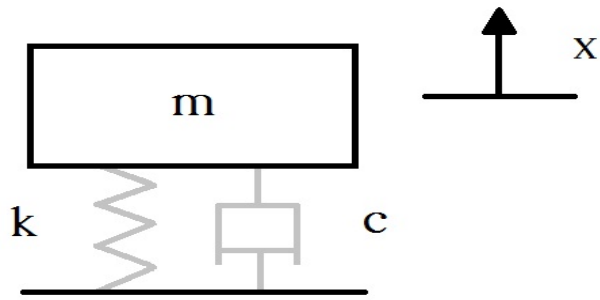

Fig. 2.3 A single harmonic oscillator

multiple DOFs. Then the equation of motion can be written in matrix form as:

$$[M][\ddot{X}] + [C][\dot{X}] + [K][X] = [F], \tag{2.10}$$

where M is the mass matrix, C is the damping matrix, K is the stiffness matrix and F is the external force. These three matrices are very important in determining the vibrational properties, including the natural frequencies and damping ratios of a structure.

If the vibration problem has a complex structure and intricate boundary conditions, it is hard to accurately define the mass, damping, stiffness matrix, as well as the loads and the boundary conditions in Eq. 2.10. It will be more straightforward to represent the complex geometry with a set of "elements". For instance, a violin top plate can be discretized to small elements as shown in Fig. 2.4 and Fig. 2.5:

Fig. 2.4 A violin top plate

Each element has its own mass, stiffness, and damping properties. By assembling the small matrices in each element into the big matrix in Eq. 2.10, all the natural frequencies

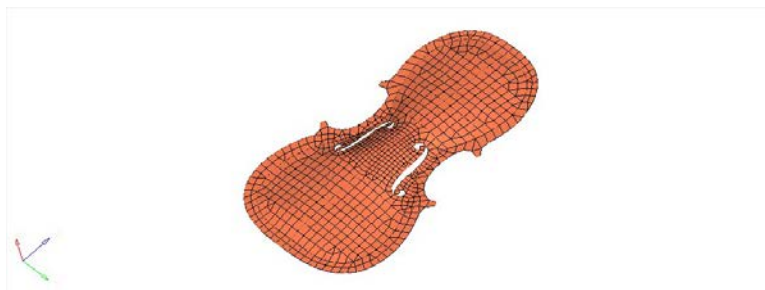

Fig. 2.5 A discretized violin top plate

and displacements at each node can be calculated.

In Eq. 2.10, all the mass, damping and stiffness matrices are square symmetric. In general, the complete equation is a quadratic eigenvalue problem. For the modal analysis, the damping terms are usually ignored. Thus we have:

$$[M]\,[\ddot{X}] + [K]\,[X] = [F]\,. \tag{2.11}$$

Considering the free vibration, in which the load on the system equals zero, the equation becomes:

$$[M]\,[\ddot{X}] + [K]\,[X] = 0. \tag{2.12}$$

It is assumed the solution has the form:

$$[x] = [a]e^{j[\omega]t}, \tag{2.13}$$

where [a] is the vector of displacement amplitudes, $[\omega]$ are the vector of natural frequencies that need to be determined, and t is the time. After substitution into the equation, this becomes:

$$([K] - \lambda[M])[X] = 0, \tag{2.14}$$

where $\lambda = \omega^2$. In order to get non-trivial solutions, the left multiplier has to be singular, so we have:

$$det([K] - \lambda[M]) = 0 \tag{2.15}$$

The eigenvalues are defined as the values of λ which satisfy the equation and can be

calculated by solving the equation:

$$([K] - \lambda_i[M])[a]_i = 0, \tag{2.16}$$

where $[a]_i$ are called the eigenvectors of the equation.

If we want to solve Equation 2.16, $[K]$ and $[M]$ must be explicitly expressed. In order to get the mass and stiffness matrices for the whole structure, the mass and stiffness matrices need to be first calculated for each element, which can be represented as:

$$[M_i] = \int\int\int_V [N_i]\rho[N_i]^T \delta V \tag{2.17}$$

$$[K_i] = \int\int\int_V [B_i]^T E[B_i]\delta V, \tag{2.18}$$

where $B_i = \frac{\delta}{\delta x}[N_i]$ is the strain-displacement matrix, N_i is the shape function and E is the elasticity matrix of element i. The value of E is related to a set of material properties, including Young's Modulus, Poisson Ratio and Shear Modulus. The elasticity matrix for an orthotropical material can be written as:

$$[E] = \begin{bmatrix} \frac{1}{E_x} & -\frac{\nu_{yx}}{E_y} & -\frac{\nu_{zx}}{E_z} & 0 & 0 & 0 \\ -\frac{\nu_{xy}}{E_x} & \frac{1}{E_y} & -\frac{\nu_{zy}}{E_z} & 0 & 0 & 0 \\ -\frac{\nu_{xz}}{E_x} & -\frac{\nu_{yz}}{E_y} & \frac{1}{E_z} & 0 & 0 & 0 \\ 0 & 0 & 0 & \frac{1}{G_{yz}} & 0 & 0 \\ 0 & 0 & 0 & 0 & \frac{1}{G_{xz}} & 0 \\ 0 & 0 & 0 & 0 & 0 & \frac{1}{G_{xy}} \end{bmatrix}, \tag{2.19}$$

where E_x, E_y, E_z are the three dimensional Young's Modulus values, $\nu_{xy}, \nu_{yx}, \nu_{yz}$ are the Poisson Ratios and G_{xy}, G_{xz}, G_{yz} are Shear Modulus values.

Since all the parameters can be explicitly expressed, the equation can be directly solved. A set of natural frequencies for each mode can then be calculated. The eigenvectors of each natural frequency, which are displacements of each node under a certain mode can also be calculated.

Consider again the bar element in Section 2.2.2, as shown below.

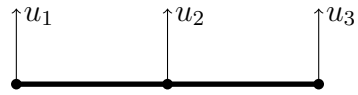

The shape function (Eq. 2.8) can be used to calculate the mass and stiffness matrices of the element. By substituting Eq. 2.8 into Eq. 2.17 and Eq. 2.18, the mass and stiffness matrices of each element can be represented as:

$$[K_1] = \begin{bmatrix} k_1 & -k_1 \\ -k_1 & k_1 \end{bmatrix} \qquad [K_2] = \begin{bmatrix} k_2 & -k_2 \\ -k_2 & k_2 \end{bmatrix} \tag{2.20}$$

$$[M_1] = \begin{bmatrix} m_1 & -m_1 \\ -m_1 & m_1 \end{bmatrix} \qquad [M_2] = \begin{bmatrix} m_2 & -m_2 \\ -m_2 & m_2 \end{bmatrix}, \tag{2.21}$$

and then assembled into the big matrix for the whole structure:

$$[K] = \begin{bmatrix} k_1 & -k_1 & 0 \\ -k_1 & k_1 + k_2 & -k_2 \\ 0 & -k_2 & k_2 \end{bmatrix}, \tag{2.22}$$

$$[M] = \begin{bmatrix} m_1 & -m_1 & 0 \\ -m_1 & m_1 + m_2 & -m_2 \\ 0 & -m_2 & m_2 \end{bmatrix}. \tag{2.23}$$

After substituting these two matrices into Eq. 2.16, the natural frequencies and the eigenvectors can be extracted. For a violin top plate, the natural frequencies and the mode shapes are important indicators that may help inform the design.

2.3 Experimental Modal Analysis

FEM can be used to calculate the natural frequencies of a structure. This technique is also called Finite Element Modal Analysis. However, “Modal Analysis” more often refers to Experimental Modal Analysis. Unlike the Finite Element Modal Analysis, which uses numerical algorithms to calculate the mode information, an Experimental Modal Analysis uses physical tests to calibrate the real structure and the mode extraction is based on the experimental data. In my thesis, modal analysis refers to Experimental Modal Analysis only.

Modal analysis is a popular technique for detecting and predicting dynamic behaviours of a structure. The modal parameters, including eigenfrequencies, damping, and mode shapes, are of the most interest and can be calculated by applying modal analysis.

The central idea of modal analysis is to get the Frequency Response Function (FRF) of the structure. FRF is the quantitative measure of the output spectrum of a structure in response to a stimulus and is often used to characterize the dynamic behaviour of the system. To compute the FRF, a measurable excitation needs to be applied to the structure at a certain position and the responses will be measured at several other positions. Subsequently, both signals are fed into an analyzer for calculating the FRFs.

2.3.1 Mobility Measurement

This important aspect of modal analysis involves measuring a set of FRFs at different chosen positions. Each FRF is defined by the ratio of the output response to the input signal. The input and the response are measured simultaneously. By applying a Fourier Transform to both the input and output signals, they can be transformed from the time domain to the frequency domain. The function will be complex. Both the magnitude and the phase can be calculated from the complex function. There are three types of FRFs with varying vibration responses: compliance FRF, mobility FRF and accelerance FRF, which correspond to displacement, velocity and acceleration, respectively in response to a force input. In my experiment, the vibration response was measured with acceleration since the accelerometer is one of the most convenient motion transducers. The equation of motion (Eq. 2.9) can then be rewritten in the form of:

$$\frac{d^2x}{dt^2} + 2\zeta\omega_0\frac{dx}{dt} + \omega_0^2 x = \frac{\omega_0^2 F}{k}, \tag{2.24}$$

where ζ is the damping ratio, ω_0 is the natural frequency, k is the stiffness of the oscillator and F is the external force. The accelerance function can be represented in the form of:

$$H(\omega) = \frac{[\ddot{x}(\omega)]}{[F(\omega)]} = \left[\frac{1}{k}\right]\left[\frac{-\omega^2\omega_0^2}{\omega_0^2 - \omega^2 + j(2\zeta\omega\omega_0)}\right]. \tag{2.25}$$

The magnitude of this function can be calculated as:

$$\left|\frac{\ddot{x}(\omega)}{F(\omega)}\right| = \left[\frac{1}{k}\right]\left[\frac{-\omega^2\omega_0^2}{\sqrt{(\omega_0^2-\omega^2)^2+(2\zeta\omega\omega_0)^2}}\right], \tag{2.26}$$

or:

$$\left|\frac{\ddot{x}(\omega)}{F(\omega)}\right| = \left[\frac{1}{m}\right]\left[\frac{-\omega^2}{\sqrt{(\omega_0^2-\omega^2)^2+(2\zeta\omega\omega_0)^2}}\right], \tag{2.27}$$

and the phase can be represented as:

$$\alpha = \pi - arctan\left[\frac{2\zeta\omega_0}{\omega_0^2-\omega^2}\right]. \tag{2.28}$$

2.3.2 Excitation

In general, the excitation applied on the structure should have sufficient magnitude and a proper frequency bandwidth of interest. There are many choices for excitation. Two most commonly used excitation techniques – impact testing and shaker testing – usually fulfill the need for different types of excitation forces. A new technique called operational modal analysis [30] has also been popular these years.

For impact testing, an impact hammer is used to generate a short-term excitation signal. A series of selected points are hit by the hammer. The impact hammer can excite a wide frequency range quickly and is the most widely used modal analysis technique due to its operational flexibility and low cost. However, the crest factor (the peak-to-average ratio of a waveform) in this technique is usually higher than for shaker testing, which will decrease the signal-to-noise ratio and perhaps cause some non-linear behaviours in the structure. Also, the repeatability of the measurements and potential double hits need to be considered, although they are not problems in shaker testing.

Shaker testing can produce more types of excitation forces. The structure is vibrated by the shaker at a series of selected points. This technique is often used in more complex structures. Since several shakers can be used simultaneously as the sources of input, the shaker excitation can be used for Multi-Input-Multi-Output(MIMO) analysis. However, the test setup is more complex than for hammer testing. Usually more equipment and channels are needed.

The operational modal analysis method uses the natural excitation of the structure

itself. It can be done while the structure is in operation, so that no specific boundary conditions are needed. However, only unscaled modal analysis data can be obtained, and the calculation process is usually time-consuming.

Impact excitations can produce a transient impulse signal. The maximum amplitude is at zero seconds. The bandwidth of the frequency and the duration of the impulse is determined by the mass and stiffness of both the hammer and the structure. The range of the frequency response is related to the tip material. A metal tip will have a higher cut-off frequency than a rubber tip. To do the measurement, a force transducer needs to be attached to the tip of the hammer. The measured force of an impact equals the measured acceleration multiplied by the mass of the impactor behind the piezoelectric disc of the transducer. The true force will be the measured force multiplied by the ratio of the total mass over the mass behind the force transducer piezoelectric disc. Unlike the shaker excitation, the hammer excitation does not add variable mass loadings on the structure. Thus, it is particularly good for light structures. The change of the mass loadings from one point to another will lead to modal frequency shifts at different measurement positions.

Given the lightweight nature of violins and their plates, the impact excitation is more suitable than the shaker excitation.

2.3.3 Coherence Function

In order to get more accurate results for impact testing, it is better to hit each point several times and take an average. Thus, the coherence function (as shown in Fig. 2.6) is an important criteria for judging whether a set of tests is accurate enough. It is defined as:

$$C_{xy} = \frac{|D_{xy}|^2}{D_{xx}D_{yy}} \tag{2.29}$$

where D_{xy} is the cross-spectral density (the Fourier transform of the cross-correlation function) between x and y, and D_{xx} and D_{yy} the auto-spectral density (which describes how the power of a signal or time series is distributed over the different frequencies) of x and y respectively.

Ideally, the coherence function should show a value of 1, which means the recorded impact signal of each hit is exactly the same. However, in the real case, incoherence cannot be avoided. There are usually several notches in the coherence function, usually at anti-

Fig. 2.6 A coherence function in the test

resonances of the FRF. Although the notches in the coherence function are due to the poor signal-to-noise ratio, no particular attention needs to be paid to this problem. By simply taking the average of several hits, the curve should be smooth enough. Usually the coherence is considered good if the value is higher than 0.95 at the resonances.

When choosing the test points, node points should be avoided. Hitting on a node point can cause very poor coherence.

Doing the impact test manually will nevertheless produce some incoherence since it is impossible to manually hit the plate exactly at the same point every time. In the experiment, a pendulum system was used for doing the hit instead of using hands. The pendulum can, to a great extent, avoid incoherence between two hits by providing consistent impacts.

2.3.4 Windows

Compared to the response signal length, the impulse signal generated by the impact is relatively short. Thus, a time window (a function that imposes zero values outside the chosen interval) can be useful to minimize the electrical noise and the vibrational noise of the hammer after the impact. In my experiments, the rectangular window was used for the input signal and the exponential window was used for the output signal, which will be discussed in detail in the later chapters. The window can effectively smooth the signal. A double hit is another problem that should be avoided during the impact test. It is caused by

either the lack of skill of the experimentalist, or the rebound of the structure. A double hit can not be compensated by a window function. Although a double hit can be compensated when computing the FRF, it can introduce some ripples as an artifact.

2.4 Composite Music Instruments

When choosing raw materials for making musical instruments, a variety of candidates are available to accommodate different types of instruments. For string instruments, wood is definitely the most commonly used material, from the very early masterpiece violins to the recent factory-made instruments.

Composite materials are not conventional materials for making musical instruments. However, with the development of material science, the application of composite materials have been greatly expanded due to their extraordinary behaviour and their reasonable prices. The appearance of composite musical instruments was the result of collaborations between luthiers and material engineers. During the past several decades of research and exploration, they have managed to design and manufacture various kinds of high-performance musical instruments with composite materials. Without sacrificing tonal qualities, these instruments not only have a fancy appearance but also excellent material properties in stiffness, durability, thermal expansion, and dimensional stability.

Charles Kaman was one of the pioneers in using composite materials for musical instrument design. In the 1960s, he founded a company named Ovation Instruments which was one of the first to design, make, and sell glass-fibre reinforced composite guitars. Later in the 1970s, they also built guitars with carbon fibre top plates. After years of experiments and modifications, they managed to reduce the thickness of the guitar top plate to 0.110 inches. The company believed that a thinner top plate would contribute to a better sound quality (which is also believed by many violin makers). The company also made wood necks reinforced with inserted carbon fibre layers.

Dr. John Decker was another carbon fibre guitar designer. He founded a company called Rainsong Graphite Guitars. Since the mid 1990s, the company has made a series of graphite guitars with a diverse array of body shapes and neck styles. They considered the sensitivities of woods to the temperature and the humidity, and tried to handle these problems (which exist even in the best guitars) by applying different structures of carbon/epoxy layers. Unlike Ovation Instruments, who makes “roundback” guitars, the

Rainsong company uses traditional guitar body geometries. They believe that by applying new materials to the traditional guitars, they can expand the sound volume range over a traditional acoustic guitar's limit.

In addition to their use in guitars, composite materials were also applied to other instruments in the string family. In the 1990s, Luis Leguia founded a company called Luis and Clark String Instruments, which manufactured a set of different string instruments including violin, viola, cello, and bass. According to their report, carbon fibre cellos were the hottest on the market. The choices of materials in different layers gave their cellos rich reverberations. The dimensional stability was also one of the spotlights in their design. As they said, the high tension at the bridge position usually leads to deformations of the wood plate after many years of playing. Since the carbon fibre had a much higher stiffness, the plate was more resistant to the tension, thus keeping the rich sound quality of the new instrument.

Composite materials also have an application in wind instruments. One example would be the very old traditional instrument: bagpipes. The traditional bagpipe tubes are made of blackwood. Although this is one of the most ideal materials for making wood instruments, it is quite sensitive to a change of temperature and humidity. Rob Gandara, a material engineer, founded a company called Pipe Makers Union LLC which manufactured carbon fibre bagpipes, flutes, and whistles. His products had good tonal qualities and stronger radiation than the traditional wood ones. Also, by applying a tapering diameter, his flutes had more powerful low registers than the commonly-seen silver alloy flutes.

Another company called Acrobaatti Oy/MATIT Flutes also has several flute products with different composite materials. The founder Matti Kahonen discovered that the carbon fibre flute's frequency spectrum range was richer than the traditional ones. The high stiffness of carbon fibre might lead to less energy absorption compared to other materials [31].

People at McGill University are also designing musical instruments with composite materials. Antoine Lefebvre from the Computational Acoustic Modeling Lab (CAML) made some saxophone necks with carbon fibre. People from the Structures and Composites Laboratory have spent several years exploring the possible applications of different composite materials to musical instruments. A natural fibre ukulele was first made by Steven Phillips in Professor Lessards' group [22]. This innovative ukelele was moulded in one piece directly and had good tonal quality. Several carbon fibre violin top plates were also made by dif-

ferent layer combinations. Many of them were considered “good” by a luthier after being assembled with a traditional body. Current projects in Lessard’s lab include designing a carbon fibre guitar board and an Indian drum.

Chapter 3

FEM and Modal Analysis Set-up

This chapter discusses the set-up of the Finite Element Method (FEM) and the Modal Analysis, which is used to obtain the FEM and Modal Analysis results for both the spruce top plate and the composite plates in the next chapter.

3.1 Numerical Model of a Spruce Top Plate

A numerical model of a spruce top plate was developed. If the numerical model is accurate enough, simple changes considering either the material properties or the geometrical parameters can be made to evaluate design modifications. It is far more convenient and economical to design using a numerical model than to change the geometries and material properties of the prototype and manufacture a lot of pieces.

Several Computer-Aided-Design (CAD) models were built according to the geometry and material parameters of the tested plates (Fig. 3.1). The first model was based on the spruce plate originally crafted by Peter Purich, which had neither varnish nor a bass bar. Other models, to be discussed in Chpt. 4, were based on composite plates, manufactured in the Structures and Composite Materials Laboratory in McGill University. In this chapter, the numerical simulation of the spruce top plate will be discussed. The prototype is shown in Fig. 3.1.

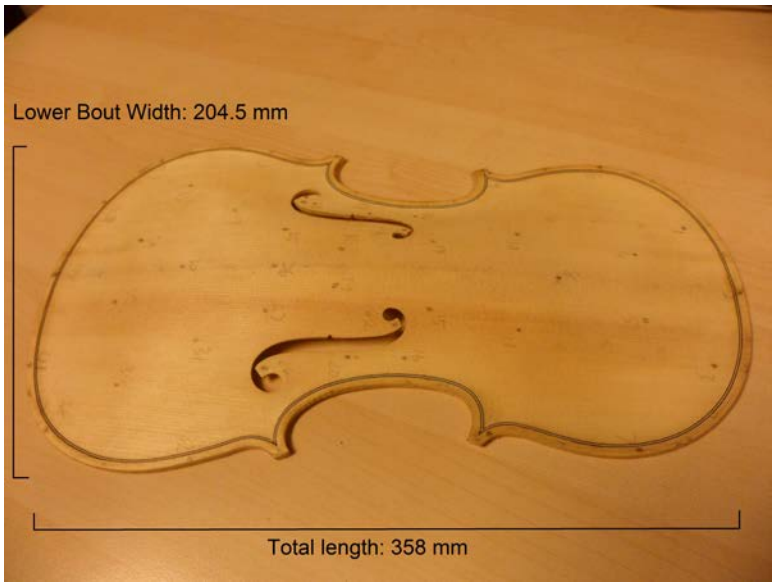

Fig. 3.1 The spruce top plate

3.1.1 CAD Model of a Top Plate

In order to build the FEM model, all the important geometrical parameters of the top plate needed to be determined first. A commercial CAD software system, SolidWorks 2012, which was available in Professor Larry Lessard's lab, was used for making the drafts on computer.

Unlike the guitar top plate, which is flat and has a uniform thickness distribution, the varying curvature of the violin top plate is hard to define. Small changes in the surface geometries can lead to large differences in the sound. Since the spruce plate from the luthier was cut and polished manually, no defined geometrical parameters were available. As a result, an electronic digital caliper (Fowler, Model EDP 13501 54-100-024-1 RS232, 24") was used to measure several feature points on the top plate. The dimensions of this top plate are defined in Table 3.1.

The arch height is also a very important characteristic feature of the top plate because it has an important influence on the bending modes and the node line positions. The arch height is measured by picking several feature points on the plate. The positions of the selected points are shown in Fig. 3.2 and the arch heights of those points are shown in Table 3.2.

The f-holes play an important role in the sound radiation of the body. Thus, the

Table 3.1 Width and length of the plate

Position of the Measured Points	Dimension (mm)
Total Length	358
Lower Bout Width	204.5
Upper Bout Width	165.5
Upper Corner Width	159
Lower Corner Width	182
Middle Line Width	108.7
f-hole Inner Notches Distance	67.3

Table 3.2 A set of selected points for defining the arch height

Arch Heights of the Points from Bottom to Top	Dimension (mm)
Point 1	0
Point 2	4.0
Point 3	9.7
Point 4	12.1
Point 5	16.1
Point 6	18.7
Point 7	17.5
Point 8	14.2
Point 9	13.0
Point 10	6.8
Point 11	0

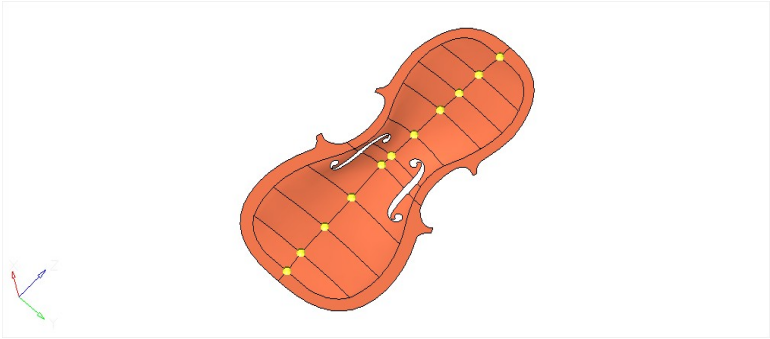

Fig. 3.2 A set of selected points for defining the arch height

positions and the shapes of them need to be defined as accurately as possible. However, the complex shapes of the f-holes make it hard to define their geometrical parameters by simple measurements. The geometries of the f-holes were borrowed from a previous model made by Hossein Mansour in CAML. The geometries of the f-holes in that model were copied into my model and projected on the top plate. Fine adjustments for the bridge position and the distance between the two f-holes were then subsequently performed.

In my model, the top plate was divided into several surfaces, with each surface governed by feature points and lines. In this manner, surfaces can be generated separately and the curvature of each surface can be controlled more precisely. In this model, reference surfaces were first drawn as shown in Fig. 3.3 (i.e. those surfaces with lighter colored lines). The feature lines in each reference surface were drawn by using the feature points in Table 3.1 and Table 3.2. Then the surfaces were generated by using these feature lines. Only half of the planes were first generated; the other half were simply drawn by reflecting the created half plane. In this manner, the model is symmetric. Note that this would not work if the plate has a bass bar.

Usually if a CAD draft for manufacturing is needed, we can make a 3-D model by extracting the 2-D model with an assigned thickness. In this manner, the model will not only look more realistic, but also contain the necessary geometry parameters for manufacturing. Different kinds of manufacturing methods can be defined based on the 3D model in the CAD software. For instance, if we want to use a lathe to cut the prototype, the manufacturing information, including the geometrical features and the cutting path, can be saved in a file and exported to a Computer Numerical Control (CNC) machine. Then the machine will automatically cut the material according to the defined path. However,

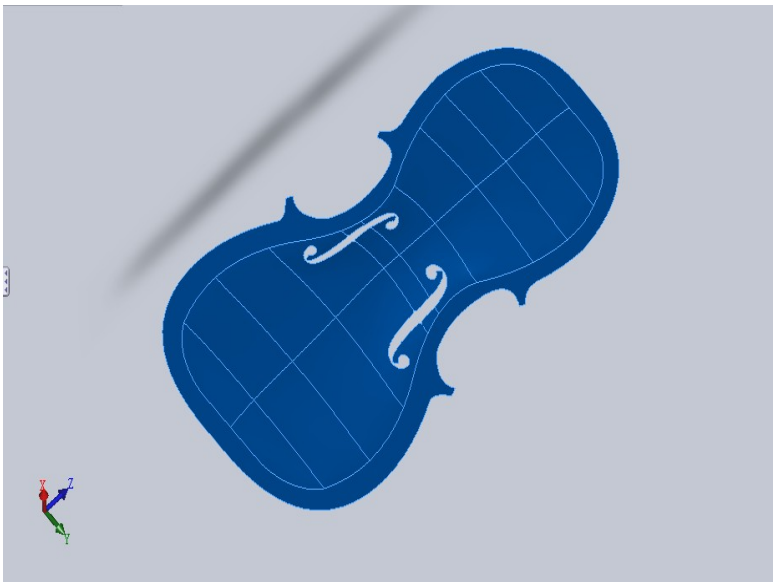

Fig. 3.3 CAD drawing of the spruce top plate

for the FEM, it is not necessary to define the geometry details of a model exhaustively. In most cases a too-detailed CAD model can even produce negative effects for Finite Element modeling because many minute features (for example, small thickness) either do not have great influence on the vibrational behaviour or are hard to model. The geometry in these areas is often too complicated if relatively coarse elements are needed to do the simulation. Of course it would be possible to apply a lot of tiny elements to the complex-geometrical areas, but the computing time will be increased significantly. One rule of thumb for doing FEM modeling is to simplify the model as much as reasonably possible.

For very thin shell structures like the violin top plates, shell elements (which are 2-D elements) are more often used than 3-D elements. In this case, it is not necessary to assign a thickness to the model. A 2-D model is accurate enough for finding the important mode parameters of the top plate.

3.1.2 Pre-Processing

The Finite Element package used for the simulation was ANSYS 10.0. It is very powerful and accurate in solving dynamic structural problems, although its pre-processing module is not very user-friendly. Thus, the pre-processing was done in another commercial software package, HyperMesh, which shares interfaces with most of the mainstream CAD software

and Finite Element software. The CAD model was first imported from ProE to HyperMesh in “igs” format. Then the model was preprocessed and was exported to ANSYS in “cdb” format.

In FEM, the first thing to consider is choosing the right element type. Applying improper elements on a model would give bad or even wrong results. In my model, shell elements were used for the spruce top plate. Solid elements were also used for the bass bar, which will be discussed in later chapters.

A shell element is the combination of the bending element and the membrane element. At each node, the shell element has both translational DOFs and rotational DOFs in each direction. When the structure’s thickness is far less than the other dimensions, shell elements can usually give more accurate results than solid elements. The reason is that a shell element has six DOFs at each node while a solid element only has three. One layer of solid elements would not be fine enough to represent the strains in the wall direction. Although accurate results can be obtained by applying enough layers of solid elements, the computation time would probably be much longer than the time needed for shell elements.

ANSYS provides plenty of elements for the user’s convenience. For quadrilateral shell elements, both 4-node and 8-node elements can be chosen. In our model, the 4-node element is fine enough to calculate the modes. The one used in the simulation for the spruce plate was Shell63, which has six DOFs at each node: three translational and three rotational DOFs in the x, y, and z directions. Since the thickness can vary continuously for this element, they were defined separately at each node.

The meshed model is shown in Fig. 3.4.

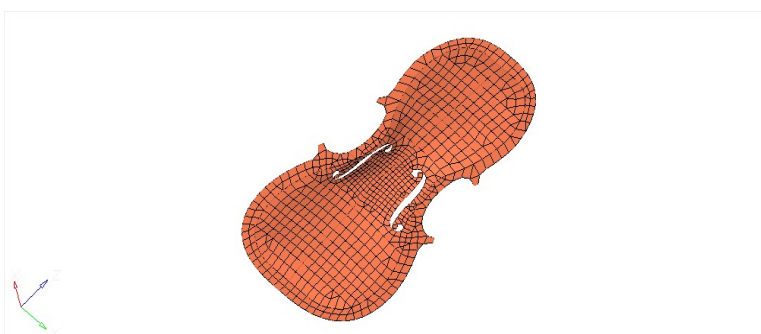

Fig. 3.4 Meshing of the spruce top plate

The meshing around the f-holes was made smaller than those at the upper bout and

the lower bout not only due to the complex geometry of the f-holes, but also due to the important modal information in the central region of the violin top plate. The meshes at the other parts on the top plate are relatively coarse in order to save computation time. Excessively fine meshing in these regions is unnecessary since the modes are less sensitive in the upper and lower bouts than at the centre area around the f-holes.

The meshes were intentionally made symmetric to ensure that the nodal displacements and the nodal lines be symmetric. To do this, half of the plate was first meshed. Then the meshing on this half plate were reflected along the y-axis. In this manner, the plot of the calculated results would be purely symmetric (although in the real case, it is hard to make symmetric nodal lines because the plate is not homogeneous).

The varying thickness of the plate was also taken into consideration. A Micrometer (Fowler EDP 10641 522-229-201-0 0-1 “MICROMETER .0001”) was used to do the calibration of the plate thickness. Several papers have discussed the influence of the thickness on the natural frequencies of the violin top plate [18, 32]; it was proven that by varying the thickness, the mode shapes can undergo changes. The meshes were divided into several regions (called ”Components” in HyperMesh) as shown in Fig. 3.5.

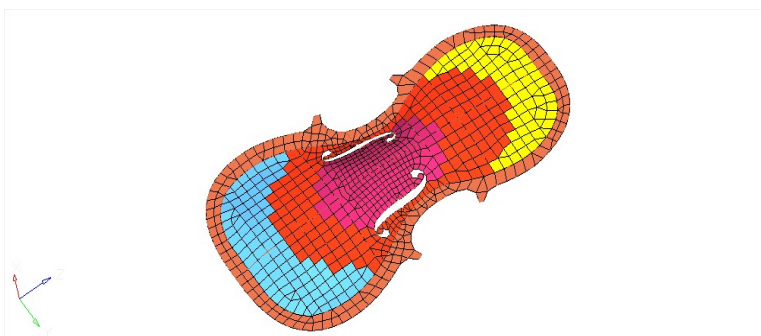

Fig. 3.5 Collectors of the top plate

The thickness corresponding to different colors are shown in Table 3.3. The thickest areas are the center and the edges. At the upper bout and the lower bout area, the thicknesses are relatively small. There are also transient areas between the center area and the upper and lower bouts. Varying the thickness is important for modeling the plate accurately.

The material properties also need to be defined. For the violin top plate, spruce is a commonly used material, and maple is more often used in making the back plate. The

Table 3.3 Arch height at a set of selected points

Arch Heights of the Points form Bottom to Top	Dimension (mm)
Brown	4.0
Yellow	3.3
Blue	3.4
Red	3.8
Pink	4.0

material properties of spruce from a previous study of the top plate was used here [4]. The results are shown in Table 3.4.

Table 3.4 Elastic parameters and density of the spruce

Parameters	Value
ρ (density)	420 Kgm^{-3}
E_x (Young's Modulus in x direction)	15.13 GPa
E_y (Young's Modulus in y direction)	1.2 GPa
G_{xy} (Shear Modulus in xy direction)	0.70 GPa
G_{yz} (Shear Modulus in yz direction)	0.059 GPa
G_{xz} (Shear Modulus in xz direction)	0.70 GPa
v_{xy} (Poisson Ratio in xy direction)	0.3
v_{xz} (Poisson Ratio in xz direction)	0.3
v_{yz} (Poisson Ratio in yz direction)	0.3

Generally, spruce is an orthotropic material which has different stiffnesses in the longitudinal and horizontal directions. The existence of grains is the cause of such difference. The relationship between the stress and the strain can be expressed by using the 3-D Hooke's Law:

$$\begin{bmatrix} \epsilon_{xx} \\ \epsilon_{yy} \\ \epsilon_{zz} \\ 2\epsilon_{yz} \\ 2\epsilon_{zx} \\ 2\epsilon_{xy} \end{bmatrix} = \begin{bmatrix} \frac{1}{E_x} & -\frac{\nu_{yx}}{E_y} & -\frac{\nu_{zx}}{E_z} & 0 & 0 & 0 \\ -\frac{\nu_{xy}}{E_x} & \frac{1}{E_y} & -\frac{\nu_{zy}}{E_z} & 0 & 0 & 0 \\ -\frac{\nu_{xz}}{E_x} & -\frac{\nu_{yz}}{E_y} & \frac{1}{E_z} & 0 & 0 & 0 \\ 0 & 0 & 0 & \frac{1}{G_{yz}} & 0 & 0 \\ 0 & 0 & 0 & 0 & \frac{1}{G_{xz}} & 0 \\ 0 & 0 & 0 & 0 & 0 & \frac{1}{G_{xy}} \end{bmatrix} \begin{bmatrix} \sigma_{xx} \\ \sigma_{yy} \\ \sigma_{zz} \\ \sigma_{yz} \\ \sigma_{zx} \\ \sigma_{xy} \end{bmatrix}. \tag{3.1}$$

In orthotropic materials, the stiffness modulus in the z-direction can be assumed to be the same as in the y-direction.

In terms of the boundary conditions, many previous studies on the guitar top plate assumed that the board was clamped at the edge [12, 33, 34]. Since the guitar has a relatively more regular geometry than the violin, the mode shapes are symmetric after assembling the soundboard on the body. Also, the top and back board of the guitar vibrates in phase. Fixed boundary conditions are assumed to predict the whole body's vibration patterns. However, the violin is a more complicated system. Neither the ribs nor the soundpost is rigidly adhered to the top and back plates (due to the attach angles). And due to the existence of the bass bar, the mode shapes are asymmetric. The sound post can also introduce a phase difference between the top and back plate. Thus, fixing the boundaries of the top plate cannot simply tell us the vibration patterns of the whole body. In my experiment, since the aim is to compare the finite element simulation results with modal analysis data of the plate, and since the boundary condition in the modal analysis is "free-free" (which will be discussed in the next chapter), the boundary conditions in the FEM model were also made "free-free". Thus, the edges do not have any constraints on their displacements.

There is no need to apply any load on the free plate since we are interested in the natural frequencies of the top plate, which are its "built-in" properties. The idea of extracting the normal modes involves solving the eigenvalue problem:

$$M[\ddot{X}] + [K][X] = 0, \tag{3.2}$$

which can be transferred to:

$$([K] - \omega_i^2[M])[X] = 0, \tag{3.3}$$

where the ω_i are the natural frequencies we are interested in.

3.1.3 Normal Mode Extraction

The preprocessed model was transmitted to the commercial FEM package ANSYS. Several matrix transformation algorithms are available in ANSYS for modal analysis, including the Block Lanczos Method, the Subspace Method, the PowerDynamics Method, the Reduced Method, the Unsymmetric Method, and the Damped Method. The Subspace Method

seems to be the most suitable algorithm for our problem. If the number of modes to solve is relatively small (less than 40), this method can give faster calculations than other methods. Also, this method is particularly suitable when the model consists of well-shaped elements. The Subspace Method uses iterations to solve full stiffness and mass matrices. It gives more accurate results than other methods.

It is not necessary to calculate all the modes for the top plate. Usually the natural frequencies below 4000 Hz are of the most interest. High frequency normal modes are very dense and difficult to differentiate. And many of them are also heavily coupled, making the mode shapes difficult to distinguish from one to another. Another technique called Statistical Energy Analysis (SEA) is more often applied for high frequency analysis.

3.2 Modal Analysis Set-up

In order to validate the results of the FEM simulation, an experimental test was conducted on the spruce plate using the roving hammer method, as a comparison. Considering the light weight of the top plate, the hammer is more suitable than the shaker as the excitation source in our experiment.

A hammer test is also called an impact test. Let's take a look at an example. If there is a structure with three points marked on it (as shown in Fig. 3.6), nine Frequency Response Functions (FRFs) in total can be calculated. It is obvious that each FRF has a different shape and that there are some peaks in one FRF which do not show up in another. If hitting at one point, the response will not be the same at different points on the structure, and vice versa. The reason is that if the excitation or response point happens to lie on the nodal line of a certain mode, the input energy might not be well transferred to excite the mode. Thus, by synchronizing several FRFs, we can avoid missing any important features in the frequency response. Ideally, if a structure has n points, at most n^2 FRFs can be extracted by roving both the hammer and the accelerometer to every point. However, such exhaustive measurements are usually unnecessary. Taking a look at Fig. 3.6, it is obvious that a synchronization of any row or column (by overlapping the FRFs, e.g. h31 + h32 + h33 or h11 + h12 + h13) can give similar results. This means that if only one row or one column of the FRFs is chosen, they will probably be enough to accurately represent the vibration behaviour of the whole structure.

In practice, people choose either to rove the hammer or the accelerometer. There is

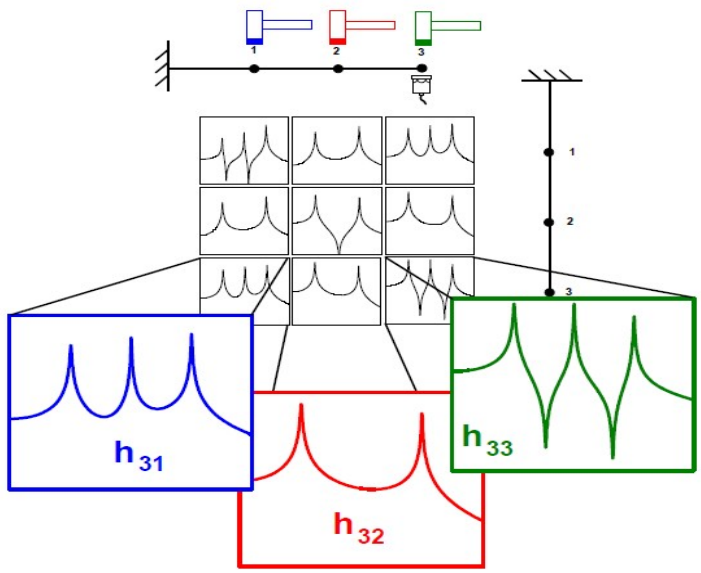

Fig. 3.6 Typical setup for a roving impact hammer test on a cantilever beam [3]

not much difference between these two choices. The idea is to choose either the row or the column in the FRF matrix. As shown in Fig. 3.6, a roving hammer test with the accelerometer fixed at point-3 is done by choosing the third row of the matrix. In my experiment, repositioning an accelerometer could be a time-consuming process because it was attached with wax. So only the hammer was roved, which was faster and easier to perform.

3.2.1 Experiment Set-up

The experiment was done in the Spatial Audio Lab in the Centre for Interdisciplinary Research in Music Media and Technology (CIRMMT) at McGill University. There are several commonly used boundary conditions for modal analysis, including free-free, fixed and mass-added boundary conditions. Among these choices, the free-free boundary condition is most commonly used, not only because it is the most easy to handle in practice, but also because it best describes the dynamic behaviour of a single component without assembly.

In my test, the free-free boundary condition was applied on the top plate. To achieve this, a nylon string was strung over a round beam near the ceiling and then attached to the top of the plate by glue. The string was intentionally made very long for two reasons.

First, using very long strings allows the top plate to be close to the ground, allowing hits to be made more easily. Second, since the movement of the swinging plate on the string is an artifact of the setup, a long length of the string can decrease these motions to very low frequencies. Generally, if the swinging frequencies are less than $\frac{1}{10}$ of the lowest body mode, they will not affect the modal information extraction. Since the frequency of the first mode of the top plate is usually about 80-100 Hz, these movements at low frequencies can be simply filtered out as noise. The whole setup of the experiment is shown in Fig. 3.7.

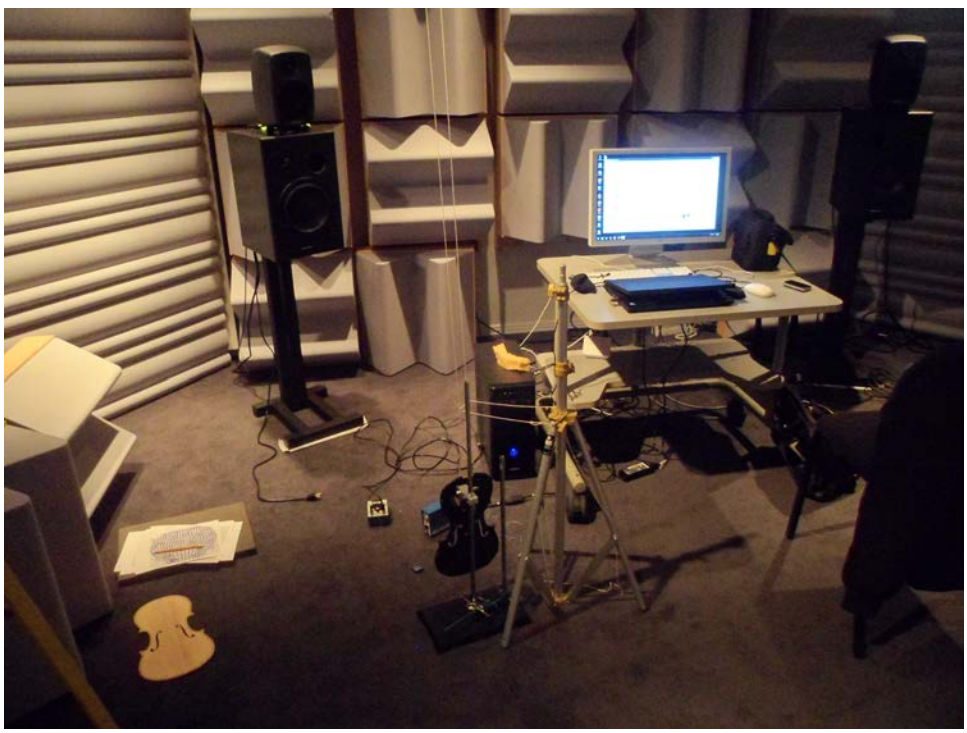

Fig. 3.7 The experiment set-up

At each selected test point, an average was taken by hitting the point several times. In a typical modal test, people often use a hand to hold the hammer and hit the selected points manually. However, this will nevertheless introduce some differences between each hit.

In order to make each hit each time as similar as possible, a pendulum system was introduced in our experiment. The top of the hammer handle was clamped in the pendulum. The rotational axis of the pendulum was perpendicular to the hit direction of the tip. The

pendulum was clamped on a chemistry stand, so that it could be easily moved to different heights. The pendulum system is shown in Fig. 3.8.

Fig. 3.8 The pendulum system

3.2.2 The Choice of the Hammer

The hammer was also carefully chosen. Several hammers with different sizes are available in our lab. A light hammer should be used to minimize mass loading and to achieve a larger bandwidth of the result. The one used in the test was a PCB Piezotronics Miniature Impact Hammer Model 086E80. The hammer is shown in Fig. 3.9.

This hammer is the smallest in the lab, having a tip diameter of 2.5 mm and a length of 107 mm. The size is proper for providing enough impact energy on the plate, so that

Fig. 3.9 Impact Hammer Model 086E80

the modes can be well excited. A force sensor is pre-installed behind the tip, in order to record the impulse signal. The specifications of this hammer are shown in Table 3.5.

There are both rubber and steel tips available for this hammer. A rubber tip is obviously softer than a steel tip, which could generate a more "gentle" impact on the structure. However, using a soft tip made of rubber would lead to a lower cut-off frequency than using a steel tip. In some previous modal analysis research on the whole violin, people used plastic tips. George Bissinger explained this as a means to protect the violin, since many of their specimens were quite expensive (a few were even Cremona violins). The steel tip could easily leave some indentations on the spruce-made plate. Unfortunately, using soft tips sacrifices the range of the frequency response. Although we are mostly interested in a relatively low frequency range (i.e. probably below 4000 Hz) for the violin top plate, it is still necessary to widen the excitation frequency range as much as possible. In my test, the price of the plate was not a concern, thus the steel tip was chosen. In this case, a high cut-off frequency was ensured. It should be noted that the plate was not damaged during the measurements.

The impact signal was recorded in voltages and was transformed to a signal conditioner before being processed by the software. The gain of the signal conditioner which connected to the hammer was set to 1.

Table 3.5 Specifications of the hammer

PERFORMANCE	Unit
Sensitivity($\pm$20%)	22.5 mV/N
Measurement Range	222 N
Resonant Frequency	$\geq$ 100 kHz
Non-Linearity	1%
ELECTRICAL	
Excitation Voltage	20 to 30 VDC
Constant Current Excitation	2 to 20 mA
Output Impedance	$\leq$ 100 Ohm
Output Bias Voltage	8 to 14 VDC
Discharge Time Constant	$\geq$ 100 sec
PHYSICAL	
Sensing Element	Quartz
Sealing	Epoxy
Hammer Mass	4.8 g
Head Diameter	6.3 mm
Tip Diameter	2.5 mm
Hammer Length	107 mm
Electrical Connection Position	Side
Extender Mass Weight	1.25 gm
Electrical Connector	5 – 44 Coaxial

3.2.3 Accelerometer

The accelerometer measures the acceleration of the excited structure. Similar to the impact hammer, an accelerometer generates an output signal in the form of voltage. A signal conditioner was also used to connect the accelerometer and the computer in order to transfer the analog output signal to digital form. The gain of the signal conditioner was set to 100, so that the frequency response plot would have the same scale as in previous papers.

The accelerometer used in the testing was a PCB Piezotronics Shear Accelerometer Model 352C23/NC Serial LW147466, as shown in Fig. 3.10. The specifications of this accelerometer are shown in Table 3.6.

Fig. 3.10 Accelerometer Model 352C23/NC

Note that the accelerometer should be able to faithfully record the acceleration of the measured structure without distorting the amplitude and phase shift. However, if the structure has some nonlinear properties, they will also be recorded by the accelerometer.

3.2.4 Selection of the Points

For the roving hammer test, the idea is to fix the position of the accelerometer at one point and use the hammer to hit at a set of selected points. In my experiment, 43 points in total were picked from the nodes on the Finite Element model, as shown in Fig. 3.11. Since

Table 3.6 Specifications of the accelerometer

PERFORMANCE	Unit
Sensitivity (±20%)	0.5 mV/(m/s^2)
Measurement Range	± 9810 m/s^2
Frequency Range (±5%)	2.0 to 10,000 Hz
Frequency Range (±10%)	1.5 to 15,000 Hz
Frequency Range (±3dB)	0.7 to 25,000 Hz
Resonant Frequency	≥ 70 kHz
Broadband Resolution (1 to 10,000 Hz)	0.03 m/s^2 rms
Non-Linearity	1%
Transverse Sensitivity	5%
ENVIRONMENTAL	
Overload Limit (Shock)	± 98,000 m/s^2
Temperature Range (Operating)	-54 to $+121C$
ELECTRICAL	
Excitation Voltage	18 to 30 VDC
Constant Current Excitation	2 to 20 mA
Output Impedance	≤ 200 Ohm
Output Bias Voltage	7 to 11 VDC
Discharge Time Constant	0.24 to 1.0 s
Settling Time (within 10% of bias)	< 3 s
Spectral Noise (1 Hz)	14,715 (μ m/s^2)/$\sqrt{Hz}$
Spectral Noise (10 Hz)	3,924 (μ m/s^2)/$\sqrt{Hz}$
Spectral Noise (100 Hz)	1,177 (μ m/s^2)/$\sqrt{Hz}$
Spectral Noise (1 kHz)	294 (μ m/s^2)/$\sqrt{Hz}$
Spectral Noise (10 kHz)	196 (μ m/s^2)/$\sqrt{Hz}$
Electrical Isolation (Base)	> 10^8 Ohm
PHYSICAL	
Size (Height x Length x Width)	2.8 mm x 8.6 mm x 4.1 mm
Weight	0.2 g
Sensing Element	Ceramic
Sensing Geometry	Shear
Housing Material	Anodized Aluminum
Sealing	Epoxy
Electrical Connector	3 − 56 Coaxial Jack
Electrical Connection Position	Side
Mounting	Adhesive

the centre area has a complex geometry and would probably contain more mode features than the edges (which was verified by the Finite Element results), more points were chosen there. The points were also made symmetric to the y-axis, so that the mode shapes and nodal lines would also be symmetric when synchronizing the mode shapes and making the animations. A full-scale plot of the plate was printed out, and the points were mapped to the real plate, as shown in Fig. 3.11 (the red points) and Fig. 3.12. The marked points were used as references for the impact hammer.

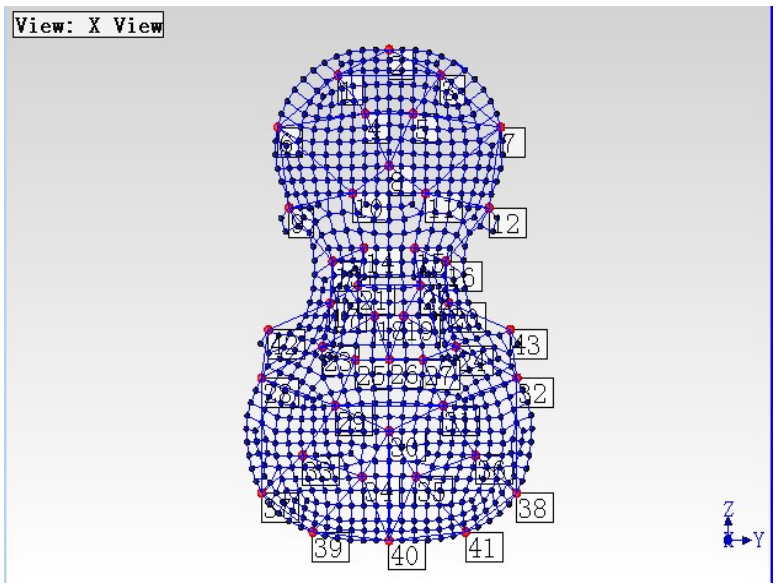

Fig. 3.11 Selected hitting points

3.2.5 Data Acquisition

The data acquisition was performed by using a National Instruments PCI-4472 8-channel Dynamic Signal Acquisition Board which was pre-installed in a PC. Since the roving hammer method was used, only two channels were needed. The hammer was connected to the input channel and the accelerator was connected to the first output channel. The board can be recognized by the modal analysis software ME'Scope 5.

At the design stage, several data acquisition methods were taken into consideration. Other choices included using a National Instruments USB-4432 4-channel Dynamic Signal Acquisition Board with Matlab code developed by Professor Gary Scavone, or using a

Fig. 3.12 Marked points on the spruce plate

sound card with a software package by George Stoppani. The advantage of using a USB-4432 card is that it can be easily connected to any PC or laptop. However, from a software perspective, only the Matlab code supports that card. Also, the data from Matlab would need further treatments. In order to animate the mode shapes, it is necessary to manually edit all the frequency response function data to a .uff file and then transmit the edited file to another modal analysis software system. Stoppani's software is able to acquire the data and do the synthesis of the mode shapes at the same time. However, the animation functions in that software are relatively weaker than ME'Scope.

Considering all these factors, the PCI-4472 Board was the final choice. The hammer and the accelerometer were connected to the first two channels of the board. The excitation and the response signals were transferred as voltage changes by the PCI board and then fed into the software for calculating the frequency response.

3.2.6 Data Analysis

The commercial software ME'Scope was used to calculate the frequency response functions and to synthesize the mode data, including the mode shapes, the natural frequencies, and the damping.

The frequency response function of each hit was calculated simultaneously upon receipt

of the impact signal. In order to minimize differences between hits, an average of 4 hits was made. The average was automatically updated after each hit, and the coherence function was also computed.

An ideal coherence function would have a value of 1 throughout the whole range of the frequency spectrum (if each hit was exactly the same). However, this is not achievable in a real experiment. There are often some notches on the coherence function, at points where the frequency response function also has notches. These notches are usually acceptable. However, if there are too many notches at other places, the data are considered bad. In my experiment, the plate was suspended by a string and each hit made the plate move a bit in different directions. In order to decrease the difference in the coherence function, it was necessary to wait a few seconds for the plate movement to dampen to an acceptable degree. Another option was to take some measures to increase the damping of the plate. In my experiment, another string was attached to the long string in order to constrain the movements of the long string. By doing this, the plate would thus move in a smaller range and return to a stable status faster. The constraining string is shown in Fig. 3.13.

One of the averaged FRFs and the coherence function in the test is shown in Fig. 3.14. As shown in the graph, the coherence function was quite smooth. Despite a few notches in the coherence, the majority of the values were close to 1. Thus, the hits at this point were considered good.

3.2.7 Modal Information Detection

After measurements at all the 43 selected points, 43 FRFs were generated. The next step was to synchronize them and extract the modal information. If all the FRFs were overlapped, several peaks would be seen on the graph, as shown in Fig. 3.15:

Important mode features can be extracted from these FRFs. The peaks on the overlapped graph are the natural frequencies of the structure. At each natural frequency, a certain vibration pattern of the plate, called the “mode shape” at that frequency, would be anticipated. The mode shape of a certain natural frequency can be calculated by using the amplitude of each FRF at that frequency. For instance, if we want to extract the mode shape of the second mode of a plate, as shown in Fig. 3.16, we can simply pick the amplitudes of the second natural frequency of each FRF and assign them to the corresponding node. Since these amplitudes are different in each FRF, the plate will be defined into a

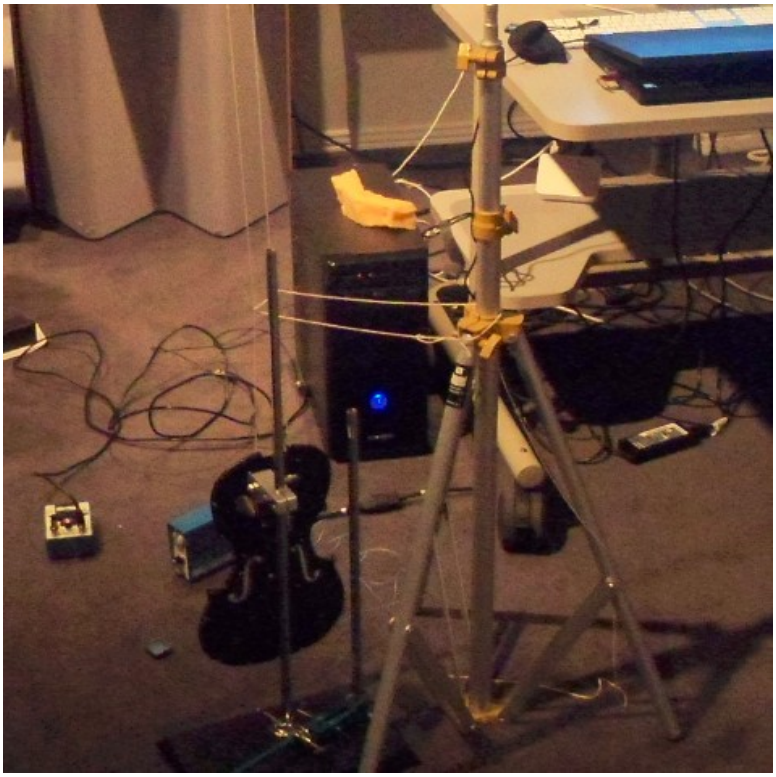

Fig. 3.13 Experimental Setup #2

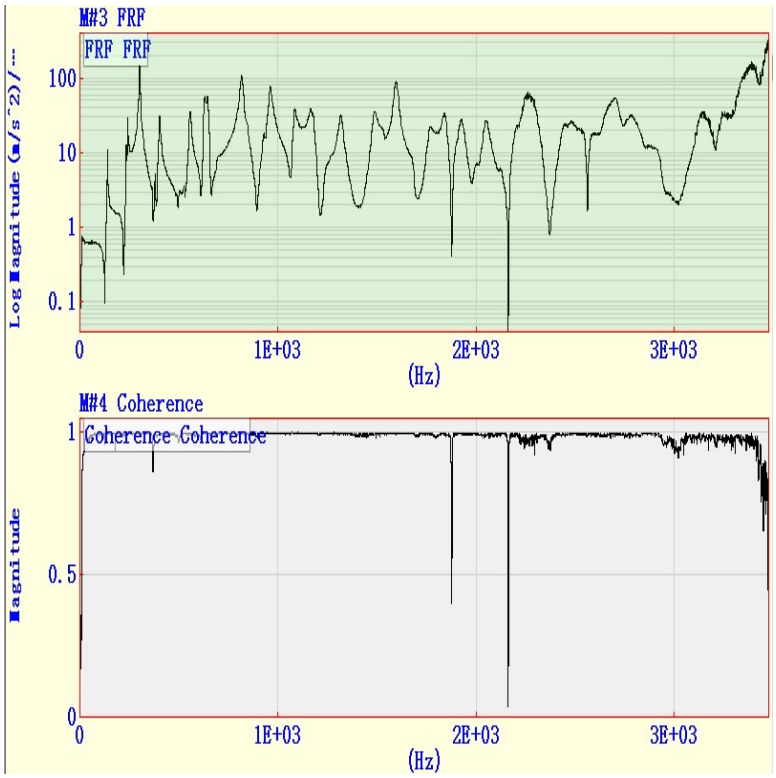

Fig. 3.14 The FRF and the coherence function of point 2

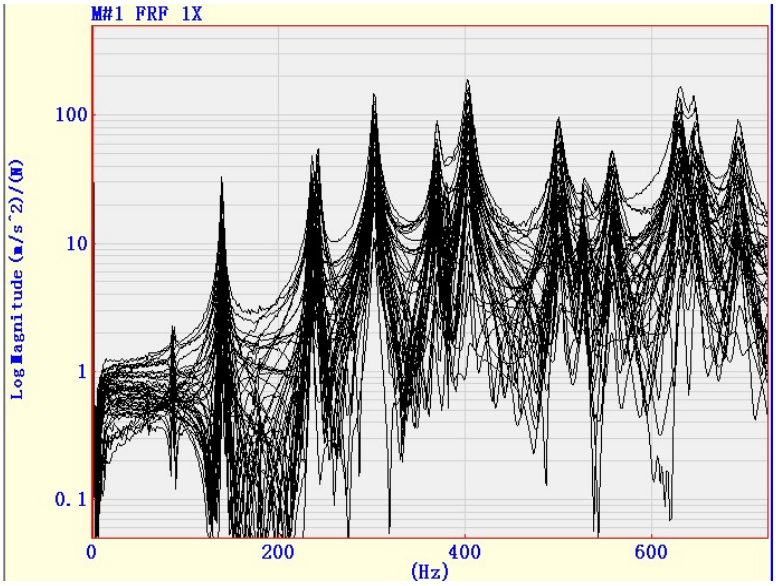

Fig. 3.15 Overlapped FRFs

physically meaningful shape. In Fig. 3.16, the plate is twisted. Thus the second mode of this plate is a twist mode.

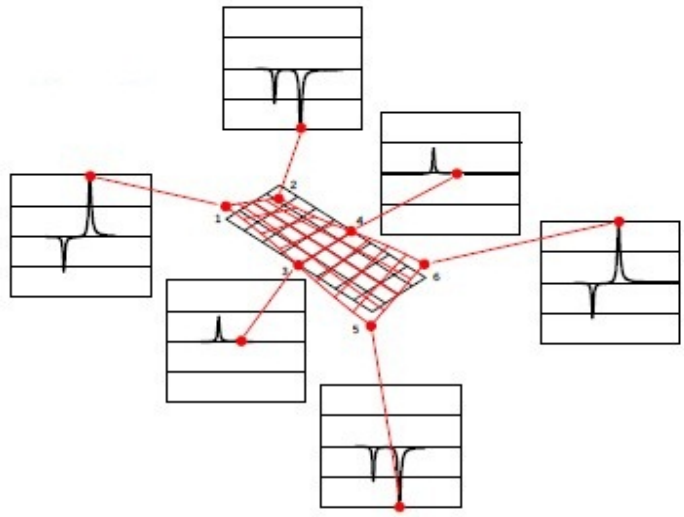

Fig. 3.16 Plate mode shape for mode 2 [3]

More intuitively, since the idea of the impact test was to hit each point and generate a corresponding FRF, the amplitudes can be considered as the response of each hit. Recall the Chladni method which stated that if the plate is governed by the second natural frequency, some areas would have large displacements (or to say, higher "sensitivities") while some would be stationary. For the impact test, if a point in the "sensitive" area is hit, more vibrations of the second mode would be excited opposed to hitting a point in the stationary area. From the frequency spectrum, we should also be able to see large amplitudes of the second natural frequency at the points in the "sensitive" area and relatively small amplitudes at the points in the stationary area. Thus, the amplitudes of the second natural frequency in each FRF can be considered as the "displacements" of each corresponding node at that frequency. In this manner, the mode shapes of each mode can be simply plotted.

In Modal Analysis, the damping values of each mode were also estimated, and it is actually a task which would have been difficult to perform in FEM. The damping values of the spruce top plate were also calculated simultaneously once the peaks were detected.

The damping ratio at each natural frequency can be expressed as:

$$\zeta = \frac{\Delta\omega_{3dB}}{2\omega_0} \tag{3.4}$$

where $\Delta\omega_{3dB}$ is the bandwidth of the 3dB decay of the peak, and ω_0 is the frequency value at the peak. For a good violin top plate, small damping ratios should be anticipated, so that the sound would not be too "dry". Comparison of the spruce plate and the carbon fibre plate will be shown and discussed in Chapter 4 and Chapter 5.

The inverse of the damping ratio can also be used, which is called the quality factor (or Q factor) to describe the damping properties of a structure.

$$Q = \frac{\omega_0}{\Delta\omega_{3dB}} \tag{3.5}$$

It should be noted that, under usual circumstances, there should not be a large disparity in the modal damping values unless there are some special damping mechanisms that affect one mode more than others. A large difference between two close modal dampings may be due to the curve-fitting error.

Chapter 4

Comparison of FEM and Modal Analysis Results

4.1 FEM Results of the Spruce Plate

The calculated natural frequencies are shown in Table 4.1. The mode shapes of the three most prominent modes, Mode 1, Mode 2, Mode 5, are shown in Figs. 4.1 – 4.3, with a comparison to the Chladni Method results by the luthier Peter Purich. As can be seen, the two set of results are in general agreement.

Table 4.1 Natural frequencies of the spruce top plate by FEM

Mode	1	2	3	4	5	6
Frequency	92.401	144.92	193.99	225.25	283.70	338.39
Mode	7	8	9	10	11	12
Frequency	407.48	430.80	468.22	552.66	566.03	672.37
Mode	13	14	15	16	17	18
Frequency	686.34	747.53	810.25	835.18	859.34	969.06

The FEM results also correspond well to those from previous papers [4, 6]. Thus, it can be proven that the FEM model of the spruce plate is reasonably accurate. The results calculated by FEM will also be compared to the Modal Analysis results in Section 4.2.

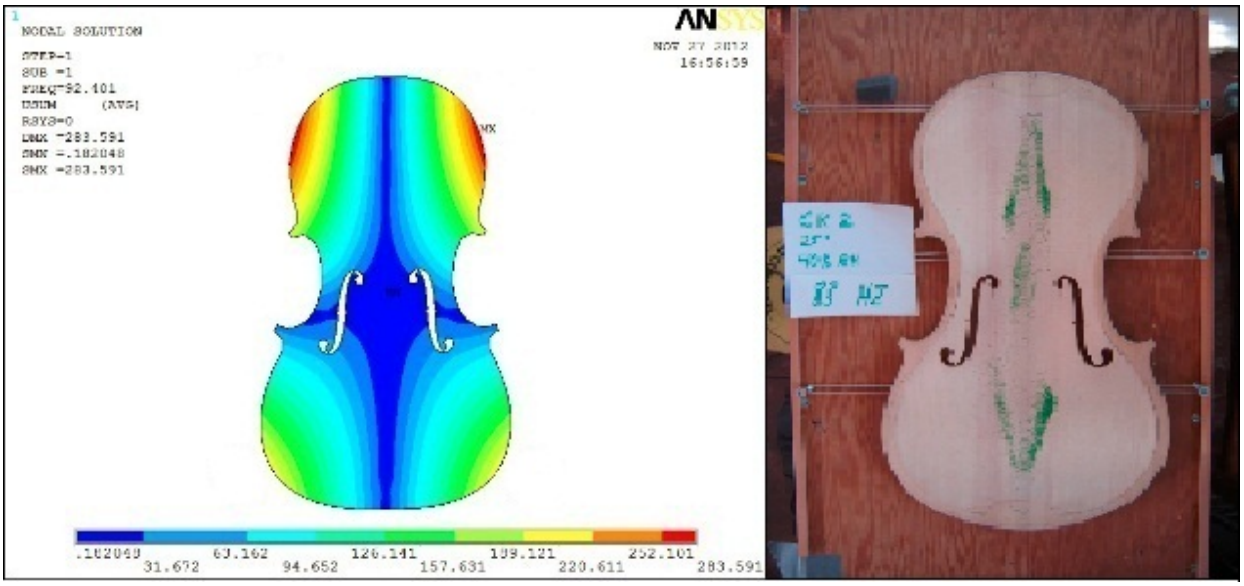

Fig. 4.1 Mode 1 of the spruce plate by the FEM and the Chladni Method

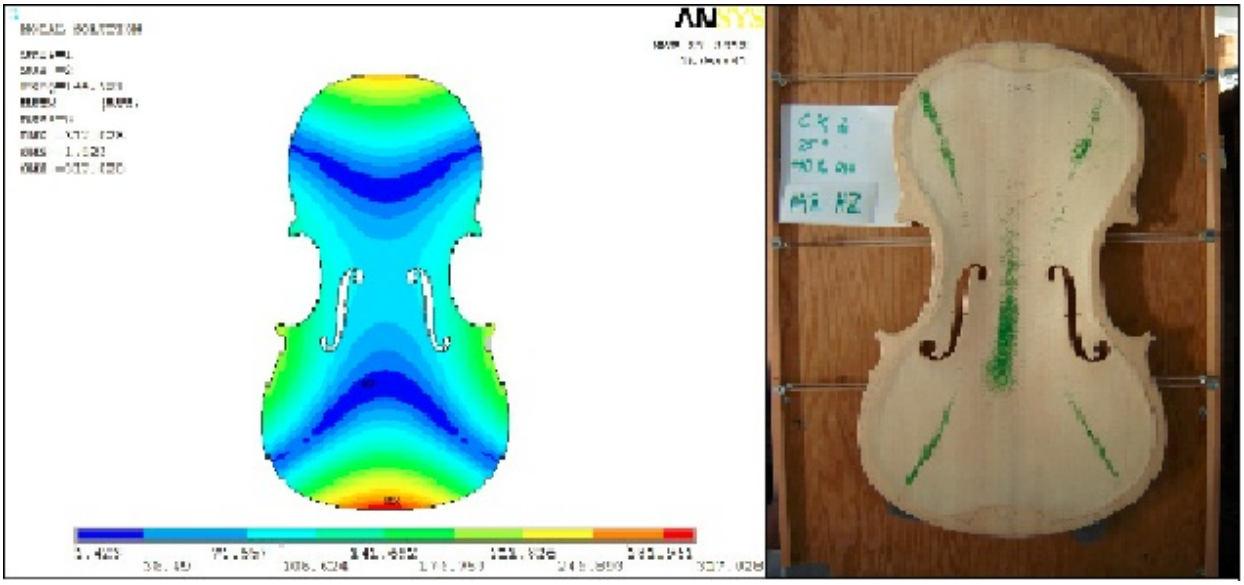

Fig. 4.2 Mode 2 of the spruce plate by the FEM and the Chladni Method

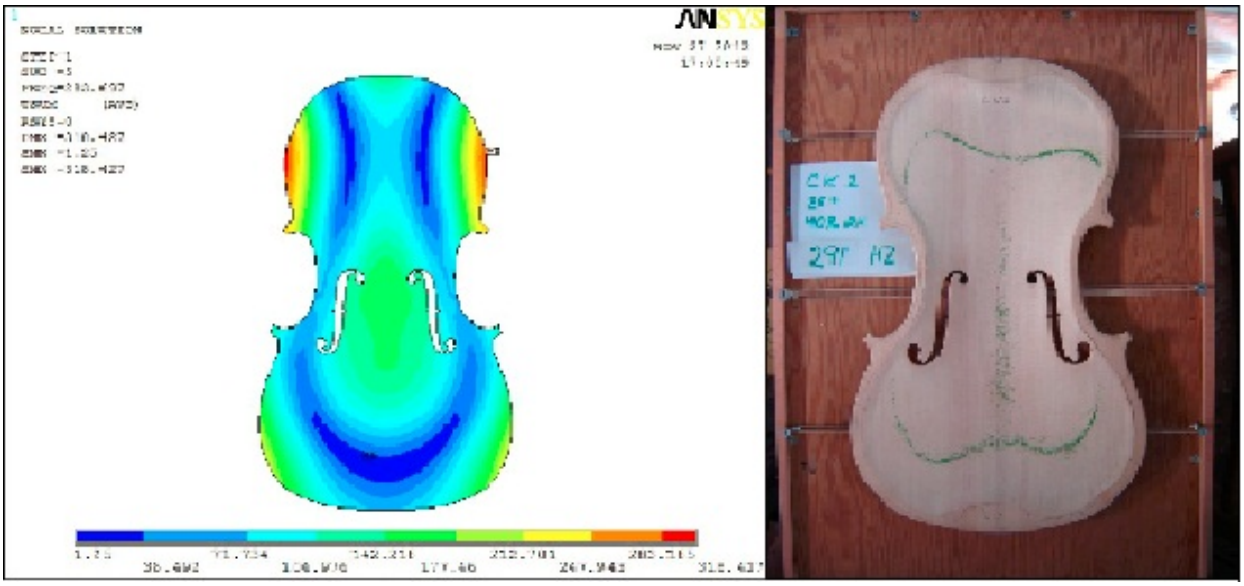

Fig. 4.3 Mode 5 of the spruce plate by the FEM and the Chladni Method

4.2 Modal Analysis Results of the Spruce Plate

In ME'Scope, the software can detect the peaks of each FRF and generate the mode shapes automatically. The first six modes of the spruce plate as determined by the Modal Analysis are shown in Figs. 4.4 – 4.9, in a comparison to the FEM results calculated previously. The mode shapes on the left side are calculated by the FEM, and the mode shapes on the right side are determined by the Modal Analysis.

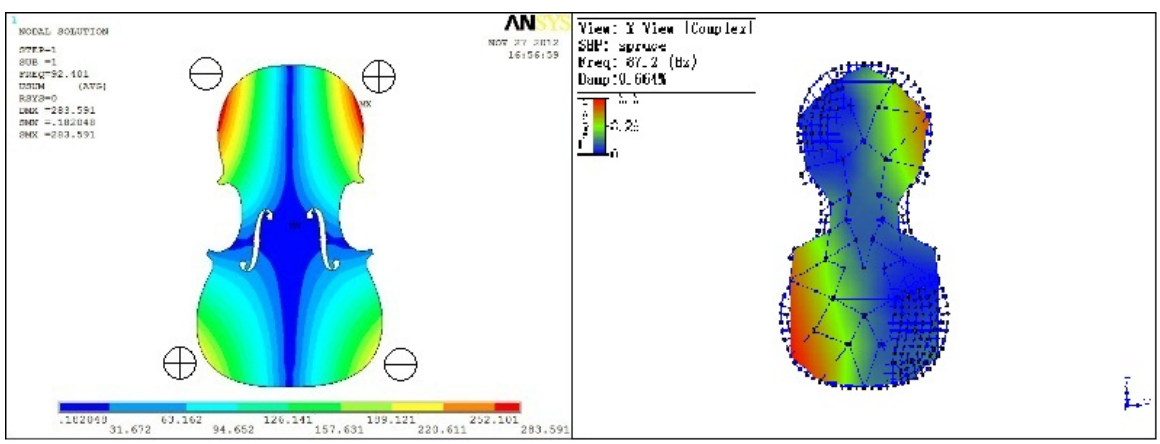

Fig. 4.4 Comparison of Mode 1 of the spruce plate by the FEM and the Modal Analysis

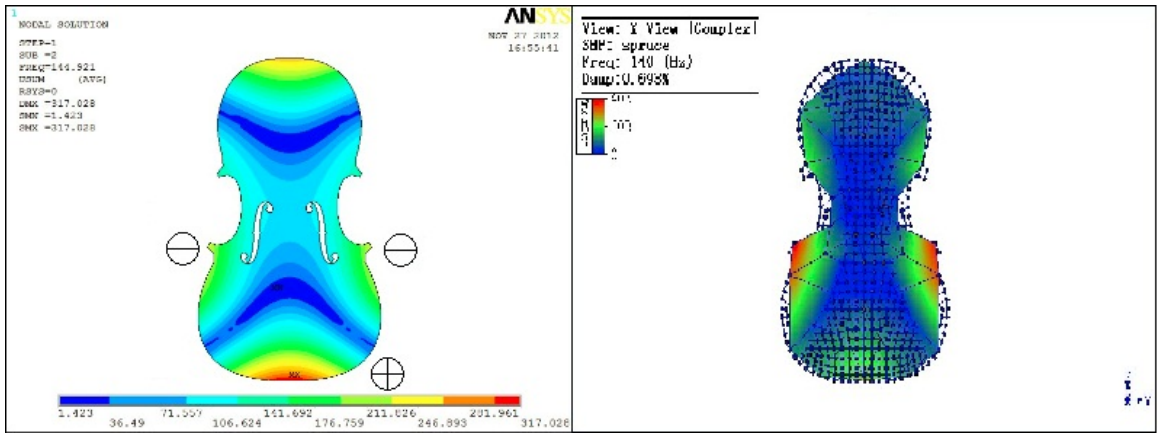

Fig. 4.5 Comparison of Mode 2 of the spruce plate by the FEM and the Modal Analysis

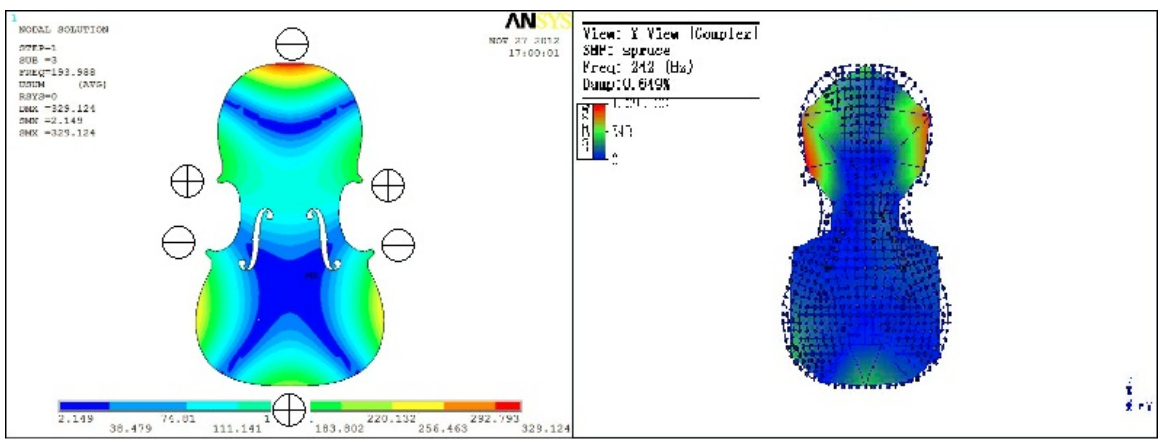

Fig. 4.6 Comparison of Mode 3 of the spruce plate by the FEM and the Modal Analysis

A list of all the natural frequencies and damping values of the modes below 1000 Hz by Modal Analysis is shown in Table 4.2:

4.3 Carbon Fibre Top Plate

Possible geometry variations of the violin have been explored for centuries. Although the current shape of the violin might already be optimal, there is still a lot of space for modifying the material properties of the violin. Composite materials are a possible alternative choice for making the violin. Considering the complex geometry of the top plate, the wood crafting

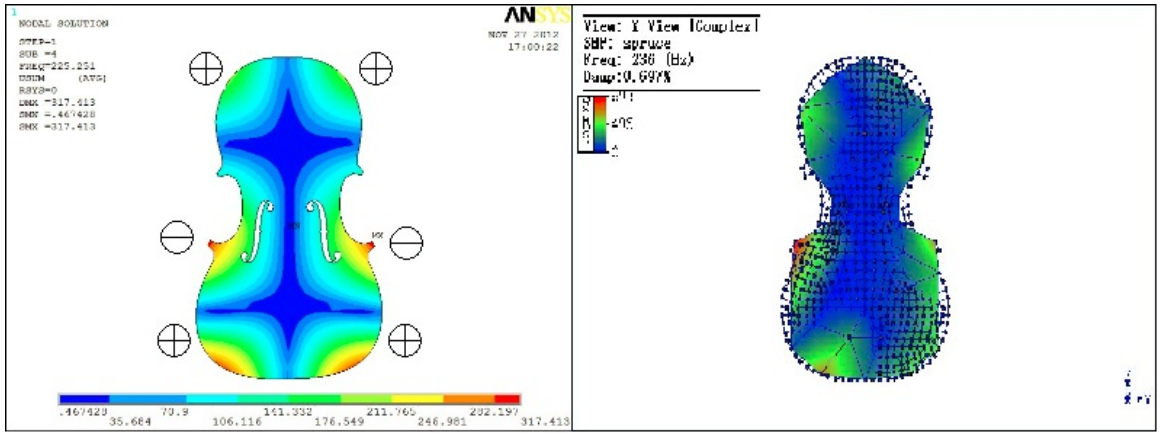

Fig. 4.7 Comparison of Mode 4 of the spruce plate by the FEM and the Modal Analysis

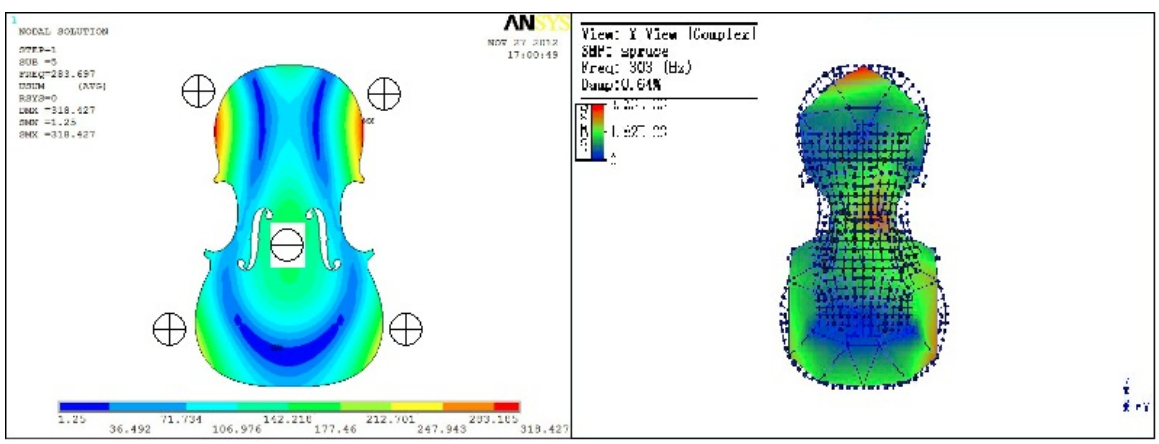

Fig. 4.8 Comparison of Mode 5 of the spruce plate by the FEM and the Modal Analysis

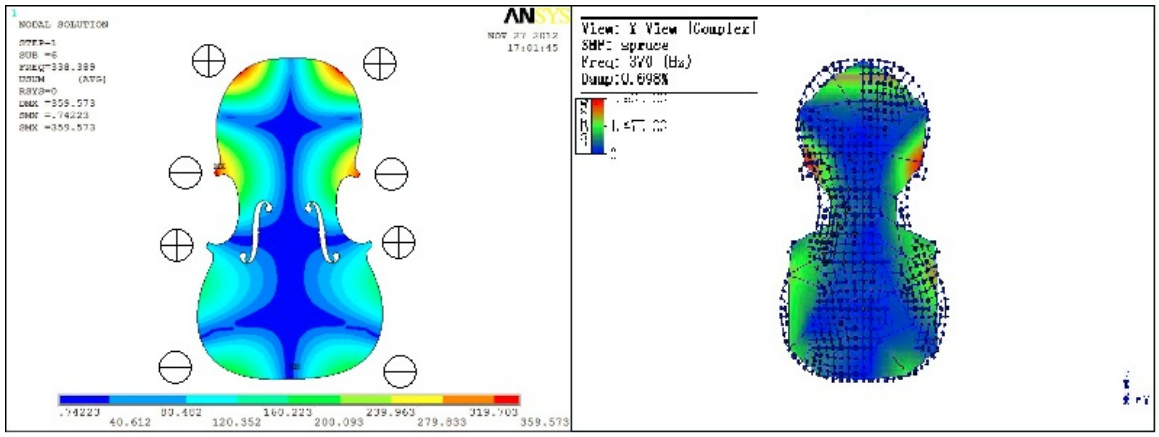

Fig. 4.9 Comparison of Mode 6 of the spruce plate by the FEM and the Modal Analysis

Table 4.2 Natural frequencies of the spruce top plate by modal analysis

Mode	1	2	3	4	5	6
Frequency	87.2	140	236	242	303	370
Damping	0.579	0.97	1.65	1.57	1.94	2.58
Mode	7	8	9	10	1	12
Frequency	381	404	501	528	558	631
Damping	2.81	2.96	3.41	3.39	3.91	4.14
Mode	13	14	15	16	17	18
Frequency	648	695	819	851	935	964
Damping	4.43	4.51	6.28	5.3	2.75	7.46

process often requires high expertise and great patience. Therefore, composite materials could be an alternative to wood because they are easier to handle during fabrication. They are also less sensitive to humidity and temperature change compared to wood, which makes the instrument more stable in different environments.

4.3.1 Choice of the Material

Many carbon fibre violin top plates were previously made in the Structures and Composites Laboratory at McGill University. As mentioned in a report from Professor Lessard's group, they paid attention to both the material behaviour and the manufacturing process when choosing the proper materials [35]. Many designs have shown good material properties but were hard to manufacture. The pieces made in this project all have sandwich structures with different materials for each layer. Some of them developed cracks, which are obviously undesirable for commercial products. The two plates from Professor Lessard's group were free of fabrication defects. The first one (we will call it plate #1 hereafter) was made up of three layers. The top and bottom layers were made of MTM45-1 epoxy matrix woven pre-preg, and the core layer was made of balsa. The second one (we will call it plate #2 hereafter) was composed of seven layers of Newport 301 unidirectional carbon fibre pre-preg and a urethane ring, as shown in Fig. 4.10. Plate #1 had a bassbar assembled on it while the spruce plate and composite Plate #2 did not.

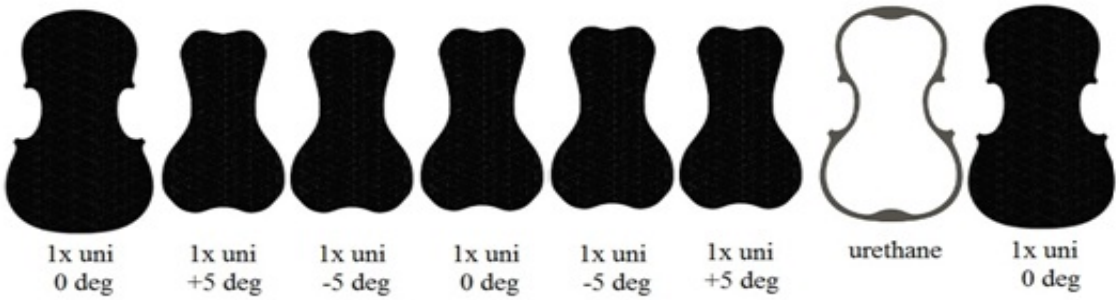

Fig. 4.10 Components of the second composite plate

Pre-preg is a terminology referring to "pre-impregnated" composite material. For this type of material, the epoxy matrix is impregnated in advance with either woven or unidirectional composite fibres. The epoxy is partially cured so that the material still has a certain degree of durability and flexibility so that it can be turned into the desired shape

during manufacturing. The pre-preg can be preserved in cold temperatures for a long time. When using pre-preg material, we first cut it into the desired shape, and then put it in the oven for several hours to fully cure it. The cure time depends on the temperature. For instance, for MTM45-1, which was used to make plate #1, the cure time is about 20 hours at 80^oC, 4 hours at 120^oC and 2 hours at 130^oC.

The whole process of making a composite plate is shown in Figs. 4.11-4.14. First, all the layers were cut and put in an aluminum mould which was CNC-machined according to the CAD drawing. Then a vacuum bag was put over the mould to extract the air inside and provide pressure (Fig. 4.11 and Fig. 4.12). Following the extraction, the mould and the materials were sent into the oven together for full curing (Fig. 4.13). After waiting for the desired time, the final prototype was ready. The violin plate was then removed from the mold and the edges trimmed slightly to its final size (Fig. 4.14).

Fig. 4.11 Stage 1 of making a composite plate (layers cut and put in mould)

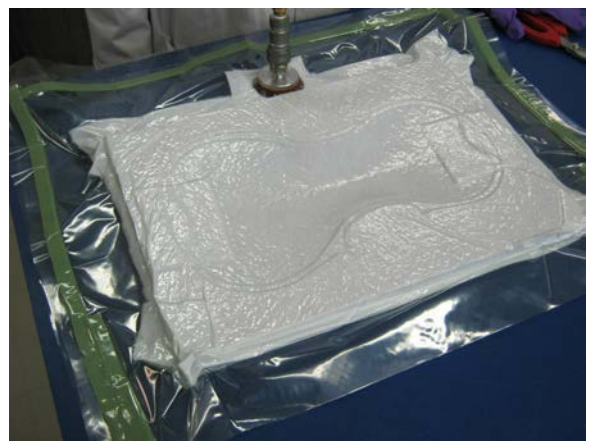

Fig. 4.12 Stage 2 of making a composite plate (air extracted)

One problem of the early prototypes was that they had sharp edges which often cut the player's neck. In an attempt to mitigate this problem, a urethane ring was also made and assembled to the top plate in the later prototypes, as shown in Fig. 4.15 and Fig. 4.16.

4.4 Numerical Simulation of the Composite Top Plates

The Finite Element Method (FEM) was applied to determine the natural frequencies and mode shapes of the two composite plates. The modeling process was quite similar to the

Fig. 4.13 Stage 3 of making a composite plate (vacuum attached)

Fig. 4.14 Stage 4 of making a composite plate (after curing)

Fig. 4.15 Stage 1 of making the urethane ring

Fig. 4.16 Stage 2 of making the urethane ring

spruce plate. The structure was first meshed, then the model was transmitted to the solver for calculation and the mode shapes were plotted finally.

The CAD model of the two plates, which was given by Professor Larry Lessard, was used to make the CNC mould. Since this model did not have f-holes in it, the f-holes were added from the spruce plate model which I had built previously and the new model was transmitted into HyperMesh for FEM Pre-Processing. Modeling Plate #1 was rather difficult because the plate consisted of several different materials. In general, the plate had a sandwich structure, with MTM45-1 weave carbon fibre pre-preg material on the top and the bottom, and a layer of wood as the core. Balsa was used around the edges and spruce was used in the central area. A bass bar, which was made of spruce, was also attached to it.

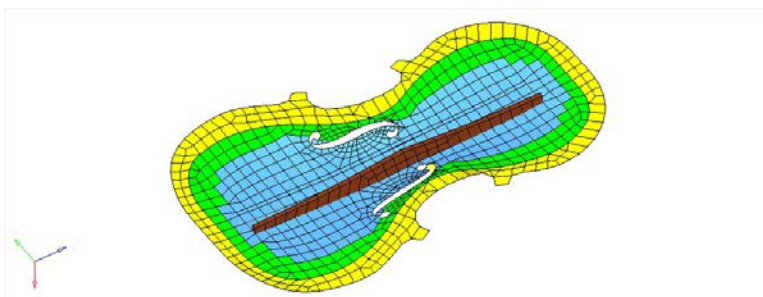

Fig. 4.17 Components of the composite plate #1

As shown in Figure 4.17, the model was first divided into several regions and named as "components" in HyperMesh. Each component was assigned with different properties. On the top plate, Shell99, a 2D 8-Node-48-DOF element, was used to model composite materials. This element allows the input material properties to be either in matrix form or in layer form. In my modeling, the layer form was used. We can define the material properties and the thickness of each layer separately. The yellow component contains three layers (MTM45-1: 0.4 mm; Balsa: 4.5 mm; MTM45-1: 0.4 mm), the green component contains two layers (MTM45-1: 0.4 mm; MTM45-1: 0.4 mm), and the blue component also contains three layers (MTM45-1: 0.4 mm; spruce: 4.5 mm: MTM45-1: 0.4 mm). The properties of these materials are shown in Table 4.3.

The bass bar was modeled with Solid45 Elements, which are 3D 8-Node-24-DOF elements. Spruce was the material of the bass bar. The joints of the bass bar and the plate were forced to have the same DOFs so that the bass bar could be considered "rigidly" glued

Table 4.3 Material properties of spruce, balsa and MTM45-1

	Spruce	**Balsa**	**MTM45-1**
Density (kg/m^3)	420	170	1600
E_x (MPa)	15130	3900	58530
E_y (MPa)	1200	600	54500
v_{xy}	0.3	0.4	0.3
v_{xz}	0.03	023	0.4
v_{yz}	0.3	0.23	0.3
G_{xy} (MPa)	700	500	2600
G_{yz} (MPa)	590	300	2600
G_{xz} (MPa)	590	300	2600

on the plate. After meshing the structure and defining all the properties, it was transmitted to ANSYS for mode extraction. The calculated natural frequencies of this plate are shown in Table 4.4. The first six calculated mode shapes by the FEM are shown in Fig. 4.18 – 4.23, with a comparison to those by the Modal Analysis. The calculated mode shapes had smaller amplitudes than the spruce plate, which may have been due to the presence of the bass bar as well as a large stiffness difference between layers. Also, the natural frequencies were in general higher than those of the spruce plate. These patterns can also be seen in the experimental results, which will be discussed in the next section. More detailed discussions about these results will be provided in the next chapter.

Table 4.4 Natural frequencies of the composite plate #1 by FEM

Mode	1	2	3	4	5	6
Frequency	77.5	149	198	269	293	358
Mode	7	8	9	10	1	12
Frequency	375	436	498	520	547	620
Mode	13	14	15	16	17	18
Frequency	647	661	687	740	759	816

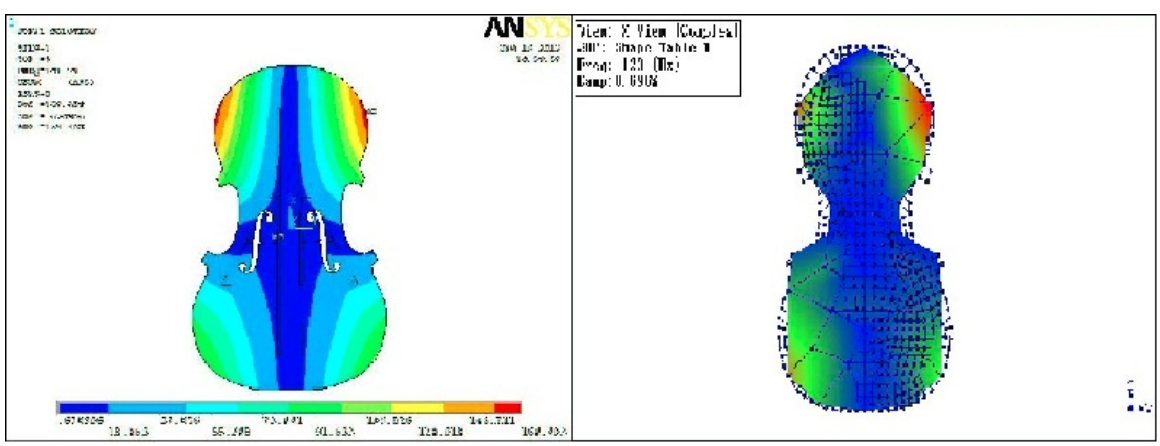

Fig. 4.18 Comparison of Mode 1 of the composite plate #1 by the FEM and the Modal Analysis

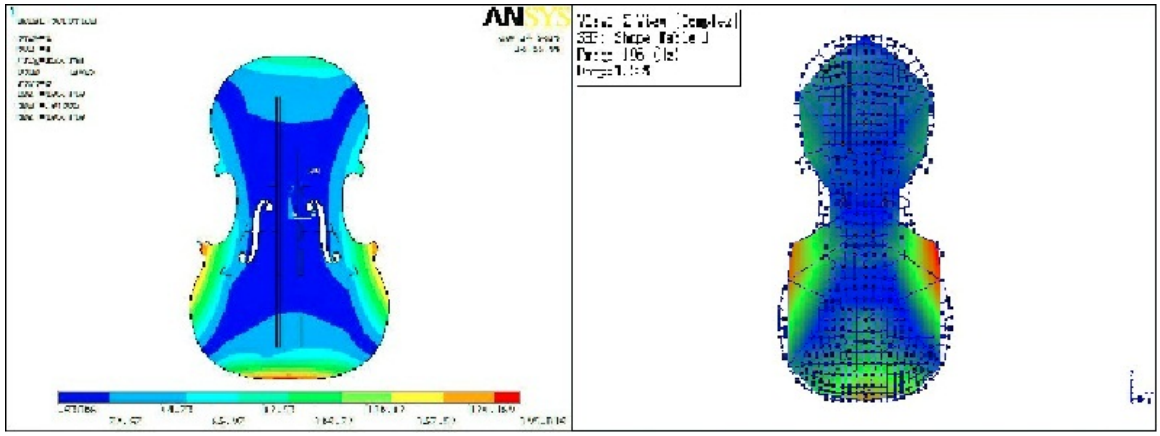

Fig. 4.19 Comparison of Mode 2 of the composite plate #1 by the FEM and the Modal Analysis

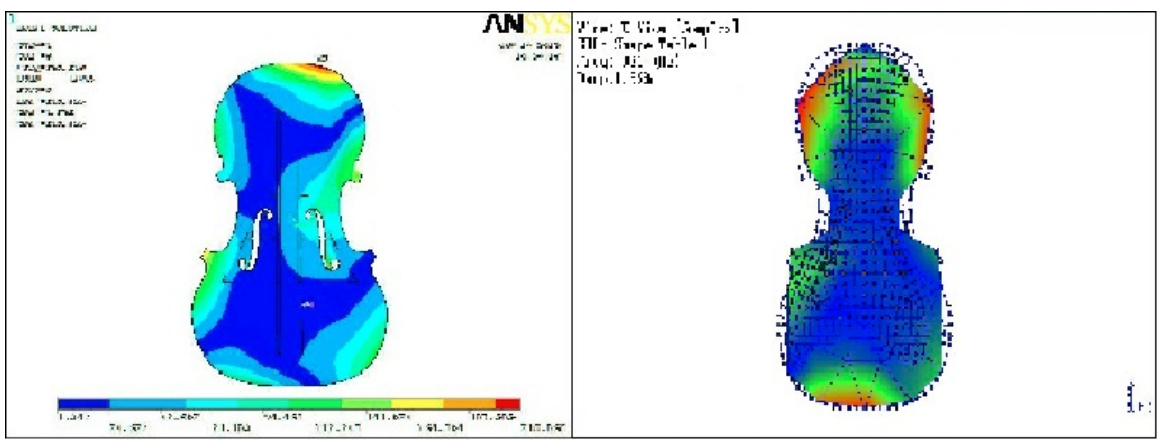

Fig. 4.20 Comparison of Mode 3 of the composite plate #1 by the FEM and the Modal Analysis

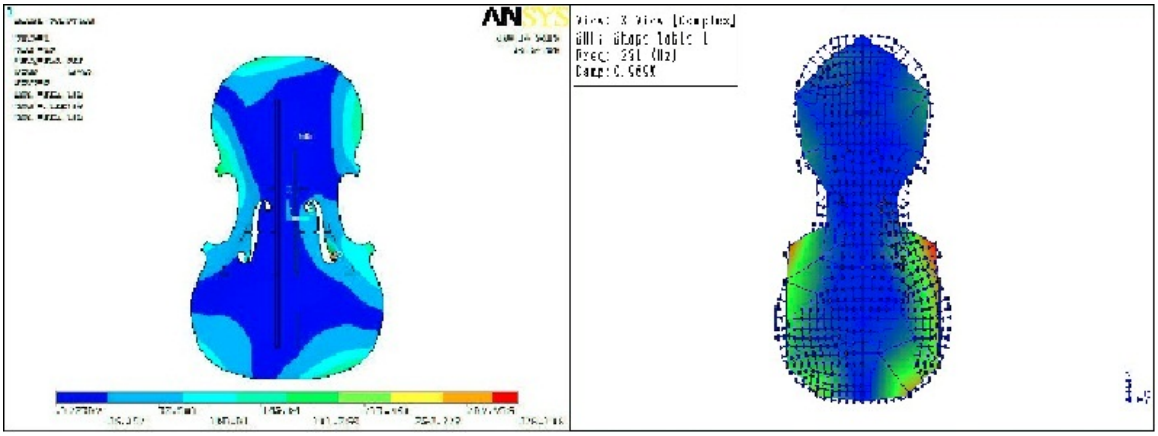

Fig. 4.21 Comparison of Mode 4 of the composite plate #1 by the FEM and the Modal Analysis

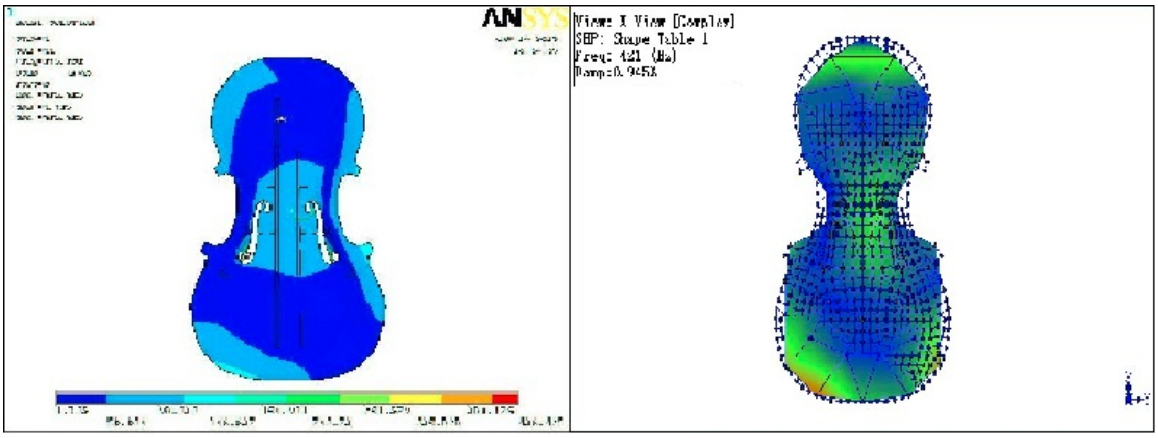

Fig. 4.22 Comparison of Mode 5 of the composite plate #1 by the FEM and the Modal Analysis

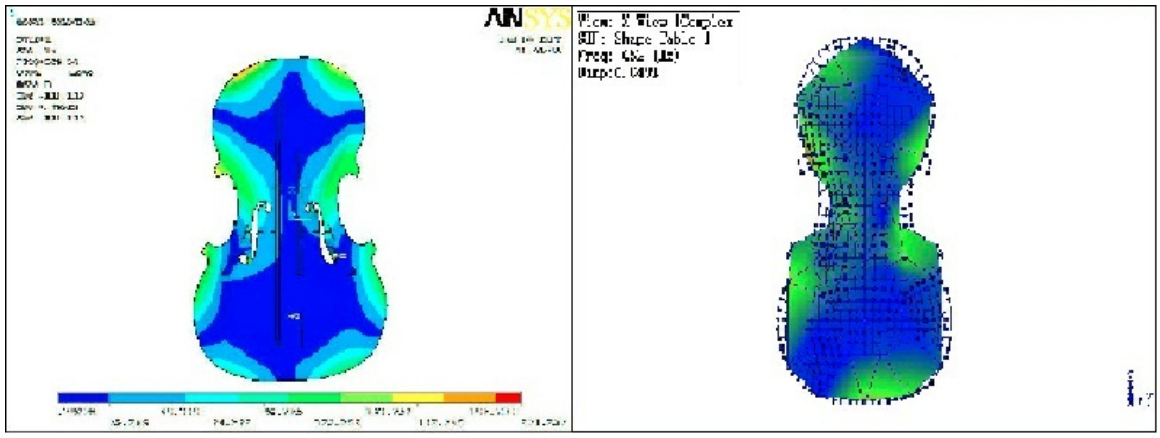

Fig. 4.23 Comparison of Mode 6 of the composite plate #1 by the FEM and the Modal Analysis

The simulation of Plate #2 was similar to Plate #1. As shown in Fig. 4.24, the blue component was made of seven layers of Newport301 unidirectional carbon fibre pre-preg material at the central part. Each layer was positioned at a different angle, as shown in Fig. 4.10. The red component contained only two layers of Newport301 pre-preg material, positioned in zero angle to each other. The yellow component marked where the urethane ring was positioned. Since there was no bass bar on this plate, Shell99 Elements was used only. By defining different layers, angles, and material properties for each component respectively, the natural frequencies can be calculated. The material properties of Newport301 and the urethane provided by the manufacturer are shown in Table 4.5. Only one Shear Modulus value (G) is provided by the manufacturer.

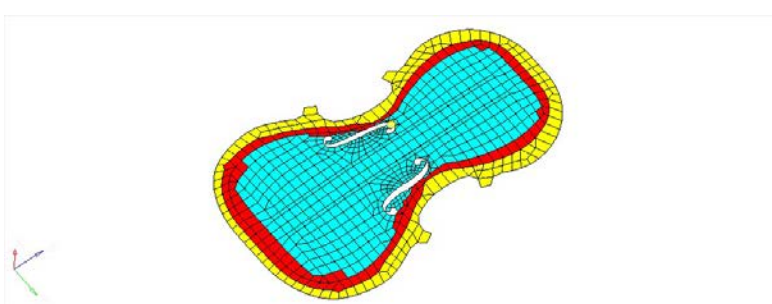

Fig. 4.24 Components of the composite plate#2

The calculated natural frequencies are shown in Table 4.6. The first six calculated mode shapes by the FEM are shown in Fig. 4.25 – 4.30, with a comparison to those by the Modal

Table 4.5 Material properties of Newport301

	Newport301	**Urethane**
Density (kg/m^3)	1227	750
E_x (MPa)	131000	7600
E_y (MPa)	8963	7600
v_{xy}	0.3	0.25
v_{xz}	0.3	0.25
v_{yz}	0.3	0.25
G (MPa)	3448	3200

Analysis.

Table 4.6 Natural frequencies of the composite plate #2 by the FEM

Mode	1	2	3	4	5	6
Frequency	49.8	108	145	183	202	249
Mode	7	8	9	10	1	12
Frequency	334	357	446	469	542	558
Mode	13	14	15	16	17	18
Frequency	648	711	800	872	907	944

4.5 Modal Analysis of the Composite Top Plates

The Modal Analysis process of the composite plates was similar to that used for the spruce plate. The test of Plate #1 was done in the Spatial Audio Lab in the Center for Interdis-

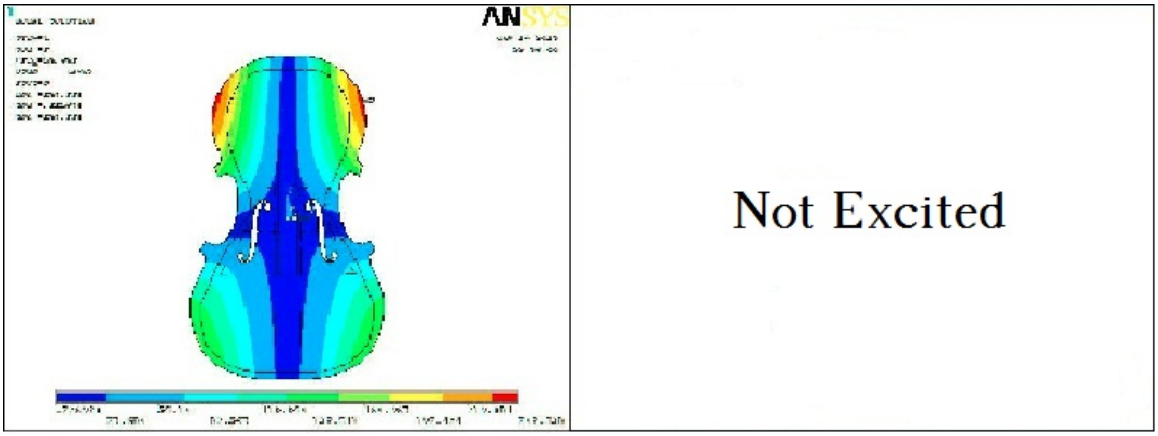

Fig. 4.25 Comparison of Mode 1 of the composite plate #2 by the FEM and the Modal Analysis

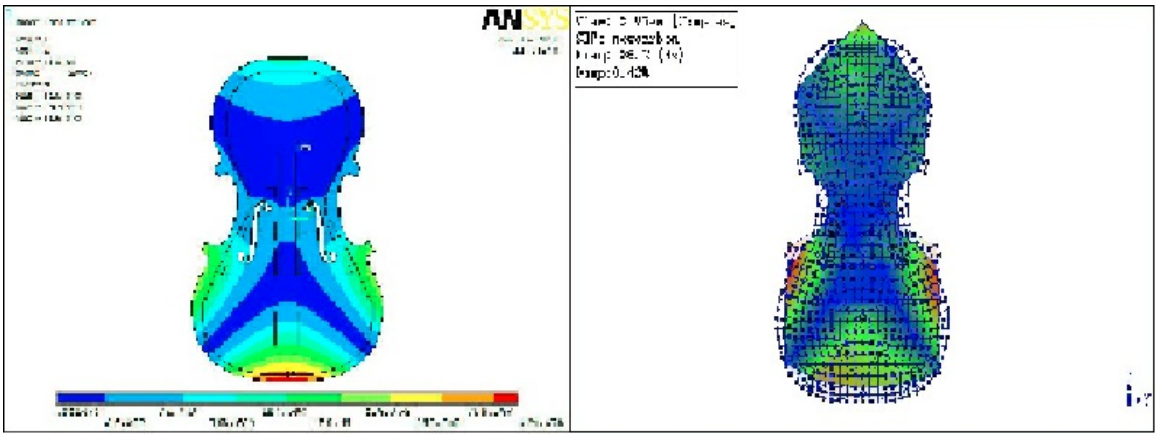

Fig. 4.26 Comparison of Mode 2 of the composite plate #2 by the FEM and the Modal Analysis

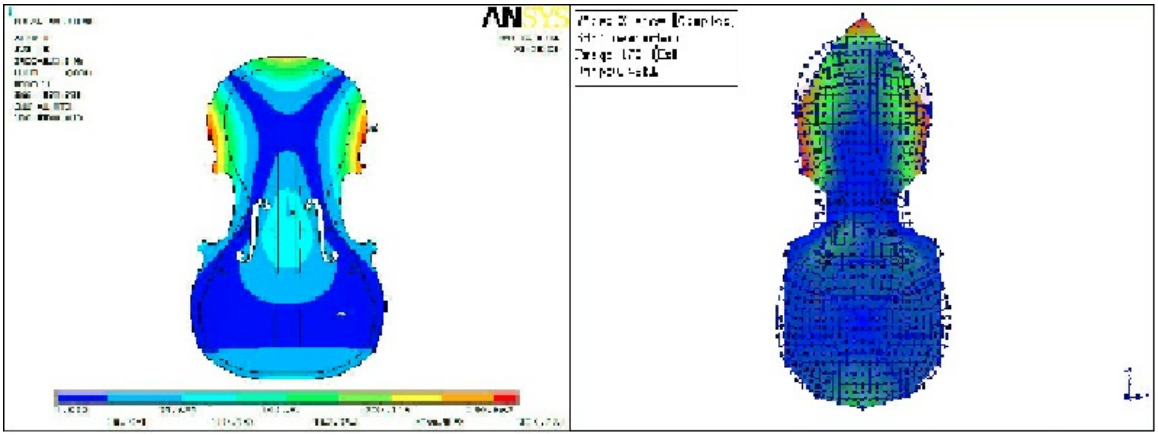

Fig. 4.27 Comparison of Mode 3 of the composite plate #2 by the FEM and the Modal Analysis

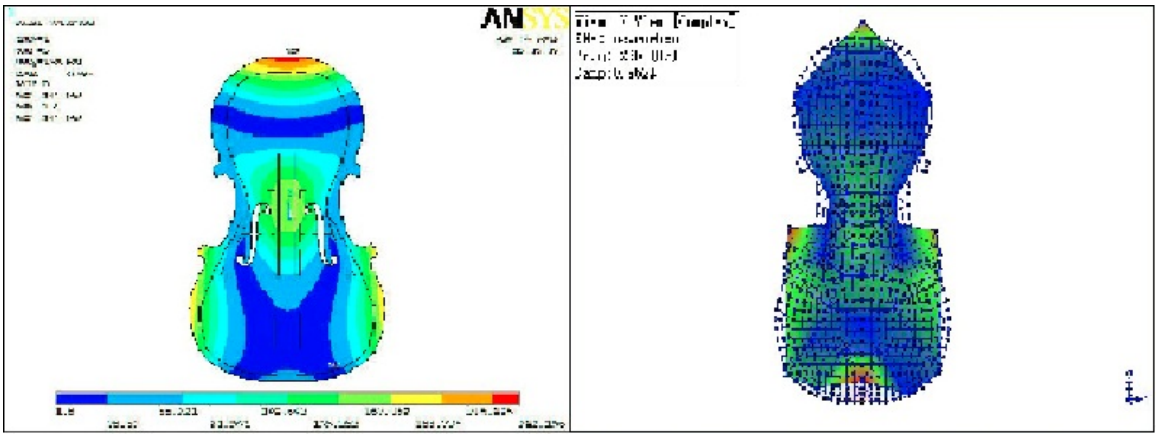

Fig. 4.28 Comparison of Mode 4 of the composite plate #2 by the FEM and the Modal Analysis

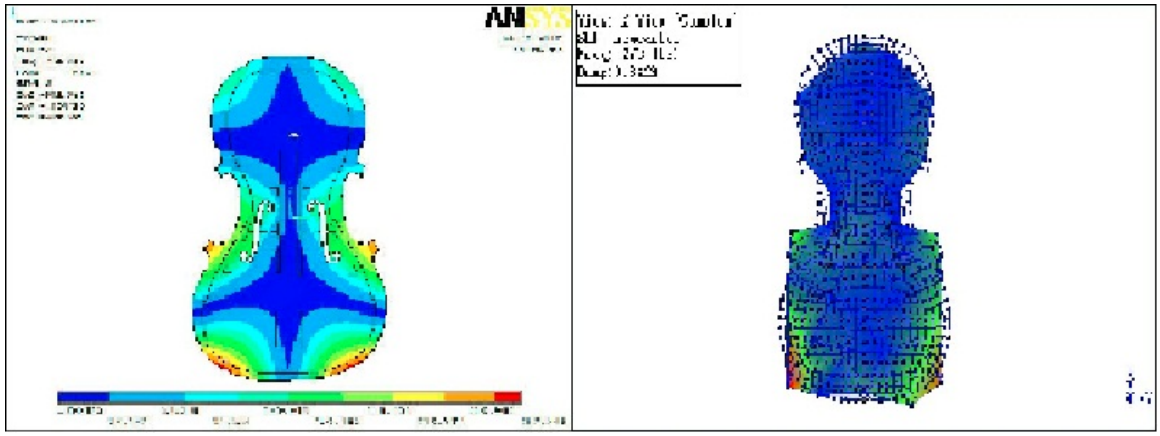

Fig. 4.29 Comparison of Mode 5 of the composite plate #2 by the FEM and the Modal Analysis

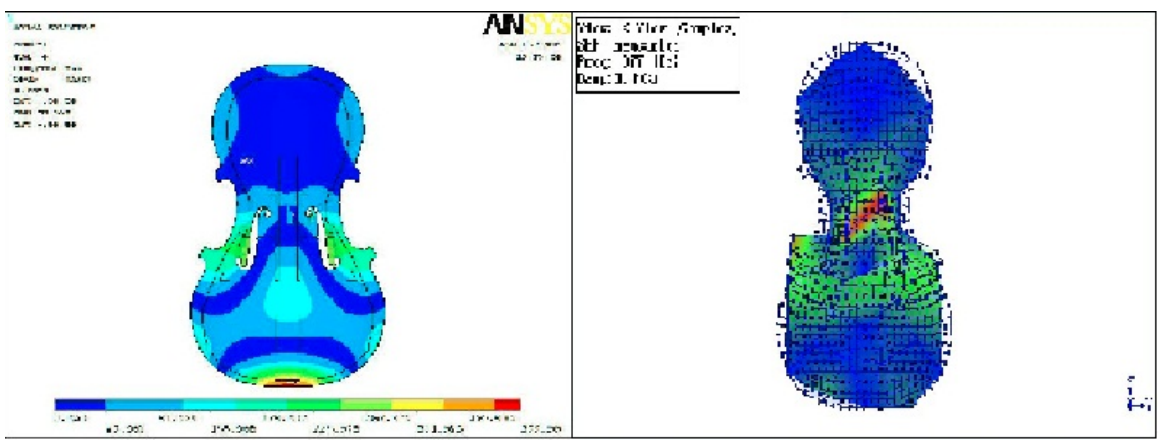

Fig. 4.30 Comparison of Mode 6 of the composite plate #2 by the FEM and the Modal Analysis

ciplinary Research in Music Media and Technology (CIRMMT) in McGill University. The equipment setup was the same as for the spruce plate, for which a roving hammer was used to hit 43 points on the plate. The synchronized mode shapes are shown in Fig. 4.18 – 4.23 and a list of all the natural frequencies and damping values below 1000 Hz calculated by Modal Analysis is shown in Table 4.7.

Table 4.7 Natural frequencies of the composite plate #1 by the modal analysis

Mode	1	2	3	4	5	6
Frequency	123	196	291	333	421	432
Damping	0.839	2.81	2.91	5.45	3.92	6.28
Mode	7	8	9	10	1	12
Frequency	452	532	625	692	704	710
Damping	4.07	8.54	3.37	2.06	0.663	0.284
Mode	13	14	15	16	17	18
Frequency	716	722	727	734	828	842
Damping	0.21	1.39	0.701	0.0475	0.592	1.28

The Modal Analysis of Plate #2 was not done at the same time as the analysis for Plate #1. Since the results of Plate #1 were quite different from the spruce plate (it was considered to have a bad tonal quality by the luthier), we decided to borrow Plate #2, the "good tonal quality" plate recommended by the luthier. Since we wanted to test the structural vibrations of the plate itself, the room condition was not really important. As Professor Gary Scavone suggested, the test was done in CAML this time, where most of the equipment was housed. The synchronized mode shapes are shown in Fig. 4.25 – 4.30 and a list of all the natural frequencies and damping ratios below 1000 Hz calculated by Modal Analysis is shown in Table 4.6.

Table 4.8 Natural frequencies of the composite plate #2 by the modal analysis

Mode	1	2	3	4	5	6
Frequency	Missing	86.2	170	236	273	377
Damping	Missing	0.362	0.844	2.27	2.29	1.48
Mode	7	8	9	10	1	12
Frequency	401	450	493	532	594	678
Damping	3.20	2.38	3.76	2.87	2.36	2.54
Mode	13	14	15	16	17	18
Frequency	732	774	804	898	937	966
Damping	3.82	3.93	4.51	5.60	7.46	5.84

Chapter 5

Discussion

5.1 FEM Results of the Spruce Plate

As discussed in Chapter 1, many researchers have studied the vibrational behavior of the violin top plate by using either FEM or Modal Analysis [9, 10, 5, 11, 4, 13, 14, 15, 16, 17]. All these studies have considered the vibrational behaviour of the traditional wooden plate. The results can be used as a comparison to the results of the spruce plate. In general, the vibration of the violin top plate contains both twisting and bending modes. The mode shapes all have similar patterns in the reference papers, although the natural frequencies differ. The results of the spruce plate's FEM simulation corresponds well with previous research.

As shown in Fig. 5.1 and 5.2, the first mode of the violin plate is a twisting mode, with two perpendicular nodal lines across the centre. The second mode is a bending mode, with two parallel nodal lines aligned in the longitudinal direction. The mode shapes of the third mode and the fourth mode are interchangeable for different plates. As can be seen here, the third mode shape in Fig. 5.1 is similar to the fourth mode shape in Fig. 5.2, and the fourth mode shape in Fig. 5.2 is similar to the third mode shape in Fig. 5.1. Similar patterns can also be found in my simulation results, in which the order of these two modes often change when changing the material properties and plate geometries. The fifth mode is usually called the "ring" mode because its nodal line has the shape of a ring. Many researchers and luthiers believe that this mode is one of the most influential on the tonal quality and that it should have an octave relation with the second mode for a "good" plate.

There is a more intuitive nomenclature for the mode shapes. The first mode, as shown

in Figs. 5.1 – 5.3, can be called the (1,1) plate mode, which means there is one node in both the transverse and longitudinal direction. Similarly, the second mode can be called the (2,2) plate mode. The third and the fourth modes correspond to the (3,2) and (4,1) plate modes, respectively. The numbers of the modes represent the half-wavelengths contained in each direction. For instance, the (1,1) mode contains half a wavelength in both longitudinal and transverse directions, while the (2,2) mode contains one wavelength in both longitudinal and transverse directions. This can explain why the natural frequency of the (2,1) mode is higher than the (1,1) mode, because the wavelength is one time shorter in the transverse direction in the (2,1) mode than in the (1,1) mode.

The fifth mode can be called (1) ring mode, the vibrational behaviour of which is different from the other plate modes. Higher ring modes should also be anticipated in the high frequency range, where more rings are present in other mode shapes.

Figure 5.3 shows the FEM simulation results of the spruce plate. The mode shapes correspond very well with previous studies [4, 5]. The calculated natural frequencies are shown in Table 5.1. The value differ a lot from paper to paper. Generally, the natural frequency of the first mode lies between 60-100 Hz. If the calculated natural frequencies are extraordinarily high or close to each other, then there may be errors in the simulation. If a model gives reasonable results, we can then simply adjust the material properties and the geometries to modify the design, which would be much faster and easier to manage than manually crafting the prototype.

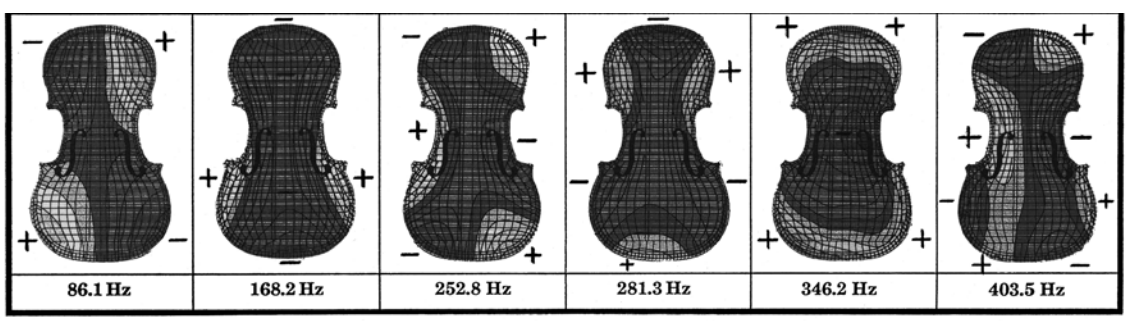

Fig. 5.1 The first six modes of the spruce plate by the FEM (Bretos) [4]

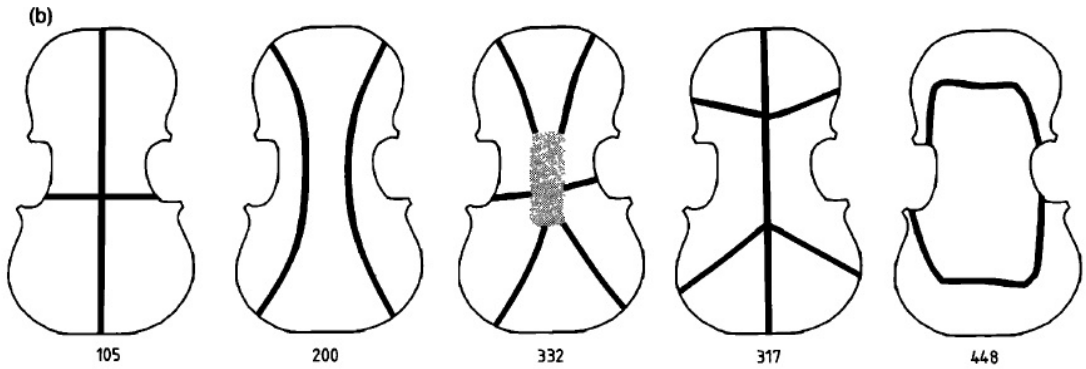

Fig. 5.2 The first six modes of the spruce plate by the FEM (Molin) [5]

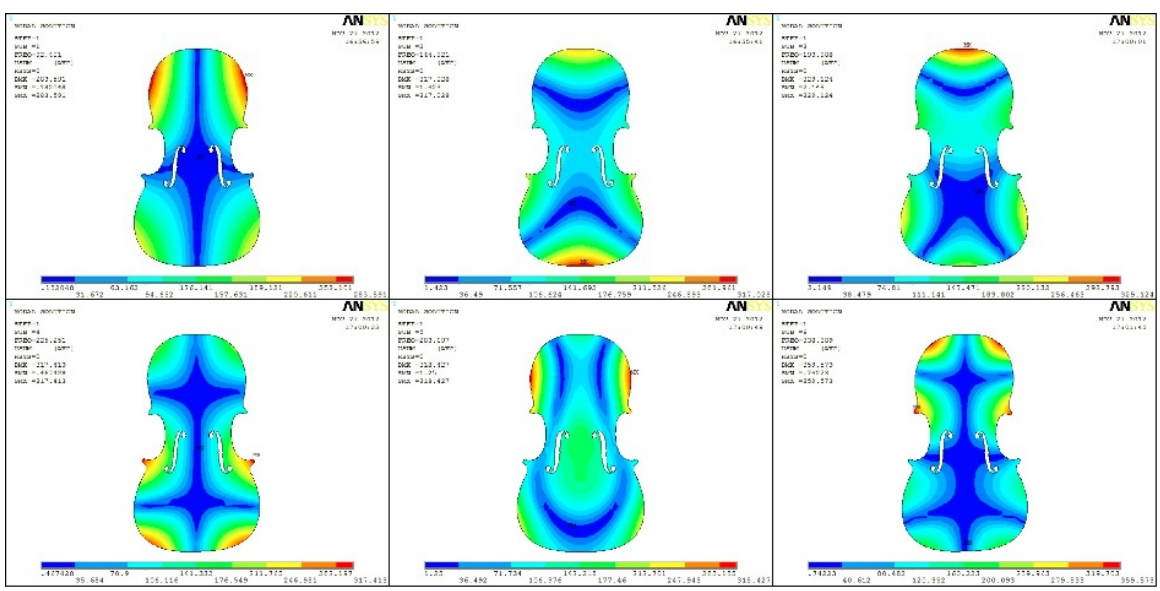

Fig. 5.3 The first six modes of the spruce plate by the FEM

Table 5.1 Comparison of the natural frequencies by the FEM of the spruce plate with previous research

	Spruce	**Bretos[4]**	**Molin[5]**
Mode 1	92.4	86.1	106
Mode 2	144.9	168.2	196
Mode 3	194.0	252.8	339
Mode 4	225.3	281.3	343
Mode 5	283.7	346.2	471
Mode 6	338.4	403.5	

5.2 Comparison of the FEM Results to the Modal Analysis Results of the Spruce Plate

The FEM is powerful for predicting a structure's behaviour. However, people might doubt whether the results are convincing enough, since the modeling process involves assumptions and any approximation or simplification of the physical condition might cause errors. Although the FEM results for the spruce plate already fit the previous research studies quite well, the modal analysis of the plate could help further validate the simulation results. Figs. 3.20 - 3.25 show the comparison of the first six modes of the spruce plate by FEM and Modal Analysis. The positive and negative signs are used to point out the moving direction of the plate. The natural frequencies of the first six modes are shown in Table 5.2. Since most of the important conclusions of violin acoustics are based on the low frequency range (and no previous papers have shown the plate mode shapes up to the sixth mode), the scope here is limited to the first six modes for comparison. As evident, both the mode shapes and the natural frequencies fit quite well comparing the two.

Now the numerical model can be considered accurate enough. We can use it as a basis for design experiments.

Table 5.2 Comparison of the natural frequencies by the FEM and the modal analysis of the spruce plate

	FEM	**Modal Analysis**
Mode 1	92.4	87.2
Mode 2	144.9	140
Mode 3	194.0	236
Mode 4	225.3	242
Mode 5	283.7	303
Mode 6	338.4	370

5.3 Vibration and Damping of the Composite Plate #1

Composite plate #1, which was made by Professor Larry Lessard's group at an early stage in their experiments with violin plates, had spruce and balsa at the core. During that stage, they mainly explored material combinations of the violin top plate which would have higher stiffness and less weight than the traditional plate. His student, Gyu-hyeong Lim, found that those plates with carbon fibre outer layers and a wooden core (including the one we used in the test) can achieve the same stiffness as the traditional wooden plate with a much thinner thickness and less weight [36].

Although the plate had extraordinary mechanical behaviour, the acoustical properties were not as desired. As judged by the luthier, Peter Purich, this plate did not produce satisfactory sounds when assembled on the violin body. Thus, one of our goals was to find the reason behind it.

The first six mode shapes of this plate, calculated by both FEM and Modal Analysis, was first compared, as shown in Fig. 4.9 – 4.16. Due to the presence of the bass bar, the mode shapes are asymmetric . This might not be too obvious in the Modal Analysis results. However, when we view the mode shapes by FEM and then compare them with those by Modal Analysis, we are able to see that they fit quite well and are all biased to one side.

The presence of the bass bar not only makes the plate asymmetric, but it also increases the stiffness of the plate. This could probably explain why the natural frequencies of this plate were generally higher than those of the spruce plate, as shown in Table 5.3. My previous experimental FEM test showed that the presence of the bass bar could increase the natural frequency of each mode by at least 10%. However, each mode showed different sensitivities to the presence of the bass bar. Some modes (e.g. the second and the third mode) had an increase in natural frequency of over 30%. From my point of view, the sensitivity of a mode is due to the mode shape itself. If the bass bar happens to stand near the nodal line (where all the points are almost stationary), the mode shape would not change much. In this case, the natural frequency would also experience a relatively small increase. However, if the bass bar happens to be near the antinodes of the mode (where maximum displacements occur), the mode shape may change a lot, hence producing even more influence on the corresponding natural frequency.

Table 5.3 Comparison of the natural frequencies by the FEM and the modal analysis of the spruce plate and the composite plate #1

	FEM of the Spruce Plate	**Modal Analysis of the Spruce Plate**	**FEM of the First Composite Plate**	**Modal Analysis of the First Composite Plate**
Mode 1	92.4	87.2	101	123
Mode 2	144.9	140	265	196
Mode 3	194.0	236	340	291
Mode 4	225.3	242	360	333
Mode 5	283.7	303	375	421
Mode 6	338.4	370	509	452

Another notable difference for this plate is the damping ratio, as shown in Table 5.4. In general, the damping ratios of each mode on this plate are much higher than those of the spruce plate (some of them are even more than twice that of the spruce plate). We usually desire small damping ratios so that the violin can be more easily excited to produce more resonances in the plate vibration. Large damping ratios would make the vibration decay fast. The sound would be perceived as “dry”, a quality which is not desired for a musical

instrument. In fact, tapping on this plate could clearly reveal that its sound was more dull than the spruce plate's. One possible cause of the high damping ratio could be the large difference in material properties between the layers, since carbon fibre is much stiffer than spruce and balsa. The high damping ratios could explain why this plate was considered to have bad tonal quality by the luthier.

Table 5.4 Comparison of the damping ratios of the spruce and the composite plates

	Damping ratio of the Spruce Plate	**Damping ratio of the First Composite Plate**	**Damping ratio of the Second Composite Plate**
Mode1	0.579	0.856	0.362
Mode2	0.97	2.7	0.844
Mode3	1.65	2.82	2.27
Mode4	1.57	5.28	2.29
Mode5	1.94	3.98	1.48
Mode6	2.58	5.88	3.2

5.4 Vibration and Damping of the Composite Plate #2

Composite plate #2, which consisted of seven carbon fibre layers, was also made by Professor Larry Lessard's group, but at a later stage. This plate, which did not have a bass bar on it, was considered by the luthier to be a good plate.

A comparison of the first six mode shapes by FEM and Modal Analysis can be seen in Fig. 4.16 – 4.21. The mode shapes agree quite well with each other even though the first mode was not excited in the experimental test. In modal analysis, it is possible to miss some modes due to the structural and material property deviations of the real prototype to the theoretical model. In general, the mode shapes of this plate were also somehow different from the previous plate. For this plate, the ring mode appeared as the fourth mode even though it usually appears as the fifth mode of a violin plate.

Since there was no bass bar on this plate, the mode shapes were all symmetric. If we

look at Table 5.5, the natural frequencies of this plate were, in general, much lower than Plate #1's; some of the modes were even lower than those of the spruce plate. The absence of the bass bar, which reduces the stiffness of the plate, could explain this. Another reason could be due to reduced thickness, which also serves a function of decreasing the natural frequencies of the plate. Plate #1 has a thickness of about 4 mm at the central part whereas the thickness of the central part of Plate #2 is only about 2.2 mm. By applying a set of FEM experiments on each plate, it was found that the natural frequencies were quite sensitive to thickness change of the plate. A thickness reduction of 0.5 mm can make all the natural frequencies decrease by about 10%, provided that all the other parameters remain constant. Thus, the low natural frequencies of Plate #2 could also be attributed to its reduced thickness.

Table 5.5 Comparison of the natural frequencies by the FEM and the modal analysis of the spruce plate and the composite plate #2

	FEM of the Spruce Plate	**Modal Analysis of the Spruce Plate**	**FEM of the Second Composite Plate**	**Modal Analysis of the Second Composite Plate**
Mode 1	92.4	87.2	65.0	
Mode 2	144.9	140	116.7	86.2
Mode 3	194.0	236	270.9	170
Mode 4	225.3	242	205.1	236
Mode 5	283.7	303	213.0	273
Mode 6	338.4	370	361.8	377

The damping ratios of this plate are shown in Table 5.4. The damping ratios are around the same level as that of the spruce plate, which means Plate #2 would have stronger resonances than Plate #1. Simply tapping on this plate reveals the difference. The low damping ratios could have been caused by the homogeneous material properties of this plate since all the layers were made of the same material. Also, the damping ratios here validated the luthier's judgment that Plate #2 possessed "better tonal quality" than Plate #1.

5.5 Comparison of the FRFs by the FEM and the Modal Analysis

The eigenvalue extraction process in the FEM can only give us the natural frequencies of the top plate. Since the mode information in the Modal Analysis was represented in the form of FRFs, it is necessary to also calculate the FRFs by FEM. Thus, we can more clearly see the transition of each mode and the peak values at natural frequencies. To do this in ANSYS, the "Harmonic Response Analysis" was applied. The idea was to add a harmonic sweep excitation on the structure and calculate the response at each node. In the numerical experiment, both the excitation and the response was defined at the middle point of the bridge. The sweep frequency range was 0-1000 Hz, which covered enough modes for analysis.

The computed FRFs are shown in Figs. 5.4, 5.6 and 5.8. Figures 5.5, 5.7 and 5.9 show a comparison of the FRFs calculated by the Modal Analysis. As can be seen, the amplitude peaks have reasonable coherence at the first several modes (below 500 Hz). At the higher frequency range (500 - 1000 Hz), the FRFs calculated by the FEM show more amplitude peaks than those by the Modal Analysis. This phenomenon is particularly obvious for the composite plate #1. As discussed previously, it is possible to miss some modes in the Modal Analysis because of the distribution of the hitting points and the manner of hitting. A main difference of the composite plate #1 to the other two plates is the presence of the bass bar, which is anticipated to have a set of natural frequencies itself distinct from the top plate. This assumption was validated by the FEM simulation of the composite plate #1. It is obvious in the animation of the FEM results that although the bass bar was adhered to the top plate, it had some featured vibration behaviour itself. In the Modal Analysis of composite plate #1, however, no point was selected on the bass bar. Thus, the Modal Analysis of this plate would not only tend to miss some of the bass bar modes, but also show less plate modes than the real case (because the bass bar can kill certain plate modes). This could potentially explain why there are less modes in Fig. 5.7 than in Fig. 5.6.

Since the modal damping ratios differed a lot for each plate, I also thought of comparing them by both the FEM and the Modal Analysis. However, the damping ratio in the FEM is an input but not output (by solving the damping matrix $[C]$ in Eq. 2.10). Thus, only the damping ratios by the Modal Analysis were presented.

5.6 FEM Experiments on Different Layer Combinations

Several parallel FEM experiments were also made to study how different layer combinations would possibly affect the natural frequencies. Professor Lessard's group had a lot of designs. Some of them were considered to have "good tonal quality" by the luthier, as shown in Fig. 5.10-5.13. Since these designs all had a similar structure to Plate #2 but with different layer combinations, the simulation was done based on Plate #2's FEM model. The results are shown in Table 5.6.

From the experimental results, it became evident that thickness played an important role in adjusting the plate's natural frequencies. Even adding a 0.3 mm layer to the plate can result in an apparent increase in natural frequencies. This further validated that the relatively low natural frequencies of Plate #2 were reasonable. From Table 5.3, it seems Plate #1 has a very different vibration behavior to the other plates, because most of its natural frequencies are much higher than the other plates. Thus, in the future design, the thickness of each layer might be restricted under a certain value, to give the desired natural frequencies. Another conclusion on Table 5.3 is that the increment of the layer number does not necessarily increase the natural frequencies. Layup 1 - 4 all have more layers than Plate #1, but with smaller natural frequencies than that plate. One should also note, that it was difficult to tell the influence of angle change on the natural frequencies from examining the extrapolated data.

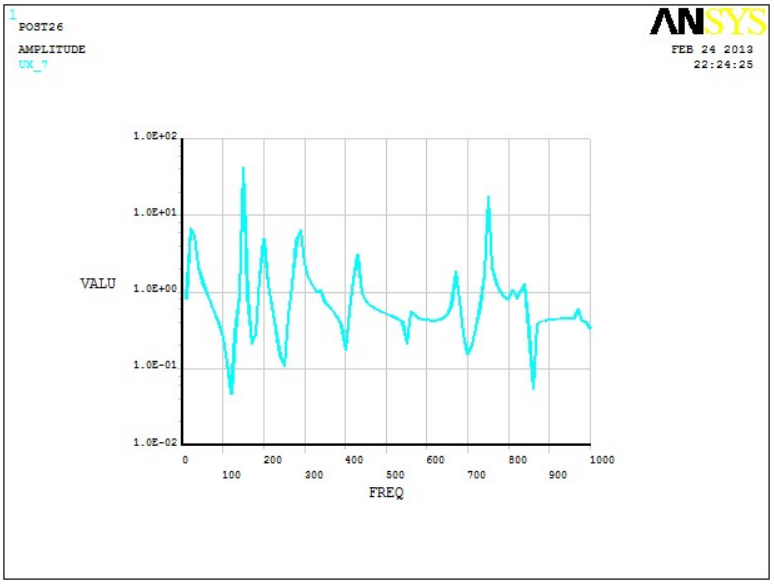

Fig. 5.4 FRF of the spruce plate by the FEM

Fig. 5.5 FRF of the spruce plate by the Modal Analysis

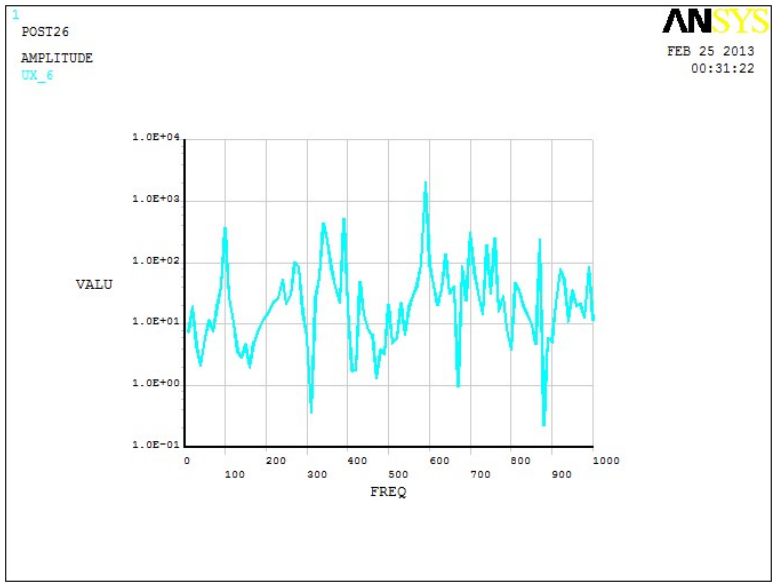

Fig. 5.6 FRF of the composite plate #1 by the FEM

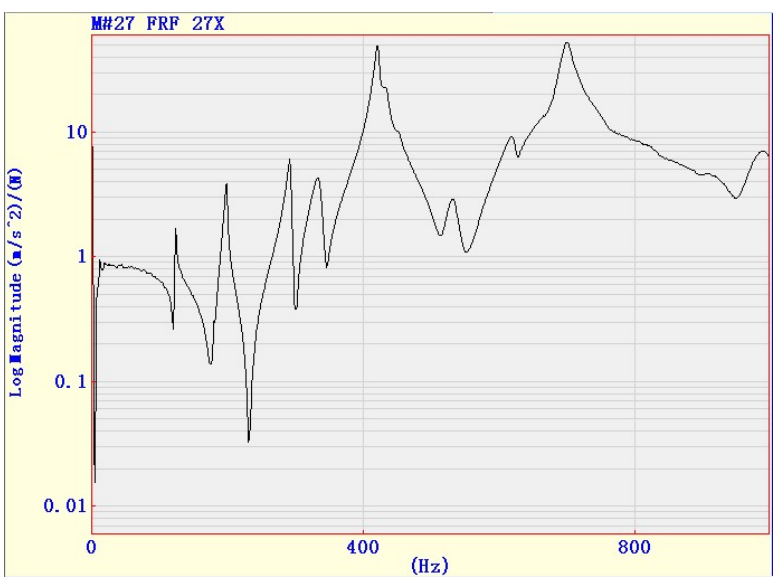

Fig. 5.7 FRF of the composite plate #1 by the Modal Analysis

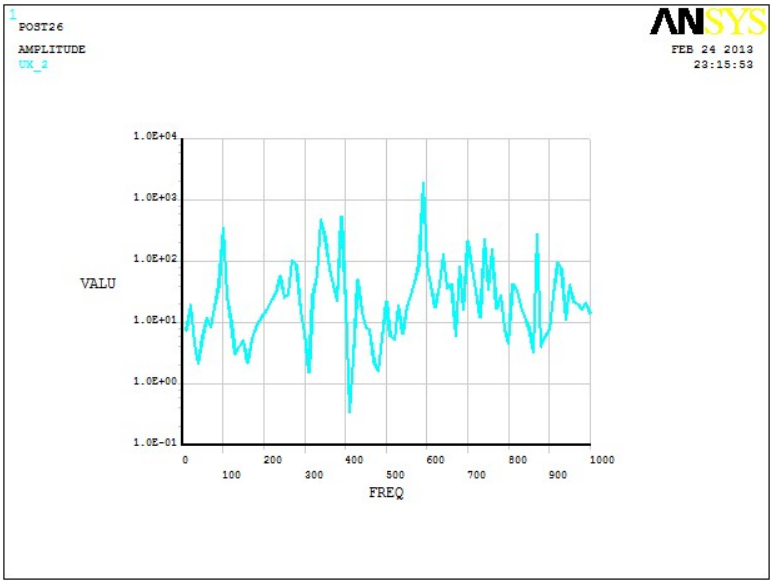

Fig. 5.8 FRF of the composite plate #2 by the FEM

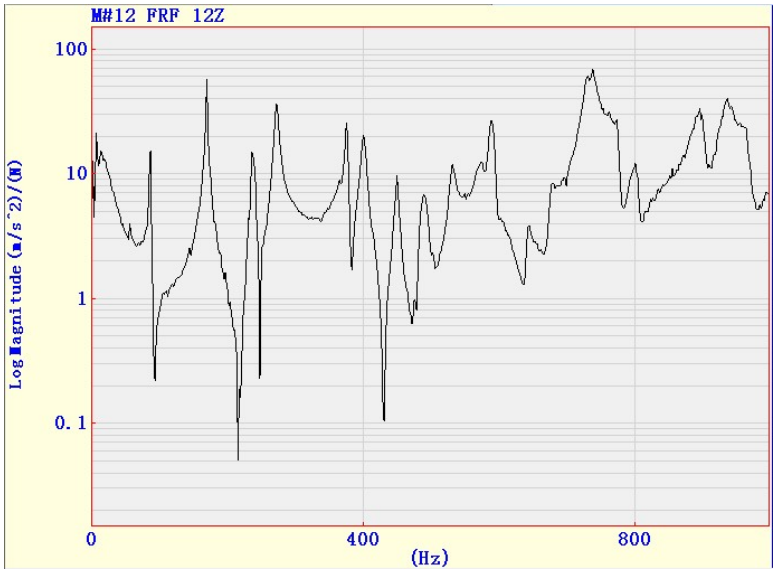

Fig. 5.9 FRF of the composite plate #2 by the Modal Analysis

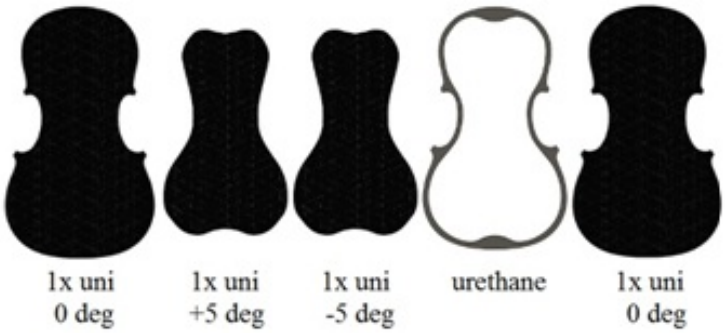

Fig. 5.10 Layup 1

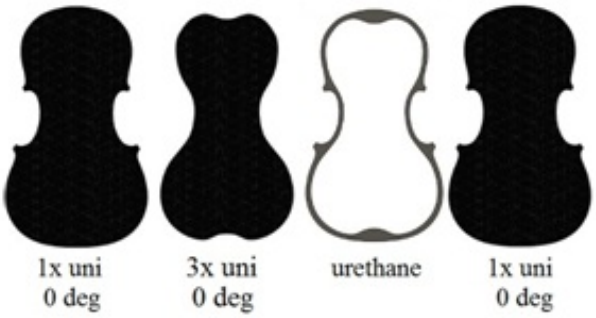

Fig. 5.11 Layup 2

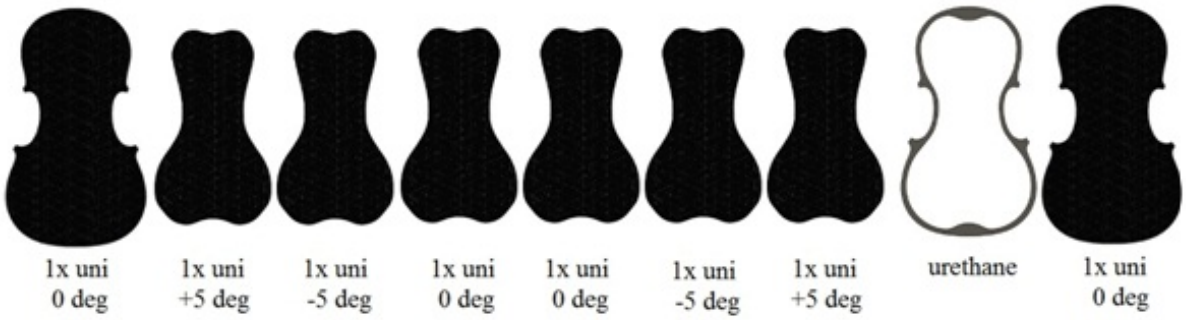

Fig. 5.12 Layup 3

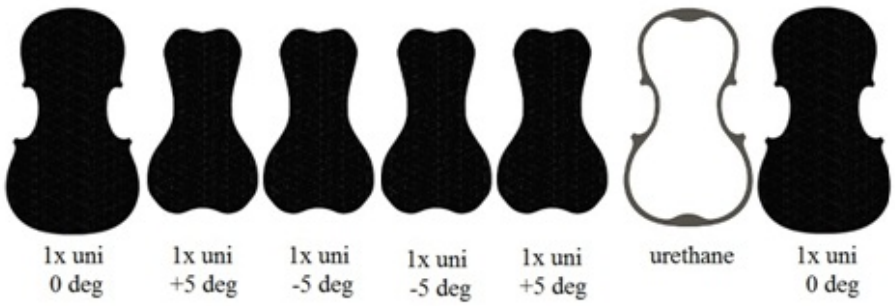

Fig. 5.13 Layup 4

Table 5.6 Comparison of the natural frequencies by the FEM of different composite plate layups

	Plate #1	**Plate #2**	**Layup 1**	**Layup 2**	**Layup 3**	**Layup 4**
Mode 1	92.4	65.0	51.2	55.2	70.3	59.9
Mode 2	144.9	116.7	92.4	100	125	108
Mode 3	194.0	270.9	143	153	181	162
Mode 4	225.3	205.1	154	172	225	187
Mode 5	283.7	213.0	160	174	233	194
Mode 6	338.4	361.8	235	256	327	279

Chapter 6

Conclusions and Future Work

6.1 Conclusions

The aim of this thesis was to study the vibrational behaviour of the violin top plate and to explore the possibility of using composite materials as a substitute for traditional wood in making the top plate. Both numerical simulations and experimental tests were applied and compared to one another, thus making the results more convincing. A violin top model based on a real spruce top plate was first built. The Finite Element Method (FEM) was applied to this model to calculate the natural frequencies and mode shapes. Then an experimental Modal Analysis was also conducted on the real plate to get not only the natural frequencies and mode shapes, but also the damping ratios of each mode. The two sets of results were carefully compared to prove that they not only fit with each other quite well but also strongly agree with many previously published works by other researchers. Thus, we can say that the spruce plate model is reasonably accurate. This model could also be helpful for luthiers who may want to modify their designs. The high coherence of the experimental results with the previous work indicates that the experiment design is appropriate.

The two composite plates were obtained from Professor Lessard in order to compare their behaviours to the traditional spruce plate. The work on these plates was original since there are no published works to date which study the vibrational behaviour of violin top plates made of new materials. Based on the results of the spruce plate, it is reasonable to believe that the modeling process and the experiment design can give meaningful results. The first composite plate (Plate #1) had wood as the core, carbon fibre as the coverage,

and an attached bass bar. The second composite plate (Plate #2) was made by several layers of carbon fibre and a urethane ring around the plate without the bass bar. Both FEM and Modal Analysis were applied again on the two composite plates. The simulation and experiment results fit well with each other for both plates. The results indicated that Plate #1 had higher natural frequencies than the spruce plate, which may have been caused by the presence of the bass bar and the large stiffness differences between the layers. Plate #1 also had much larger damping ratios than the other two plates, which was not desirable. The high damping ratio could explain why it was judged by the luthier as having "bad tonal quality." As for Plate #2, its lower thickness may have generated lower natural frequencies than that of the spruce plate. The damping ratio of Plate #2 was quite similar to the spruce plate, which could have been a reason for it to be judged by the luthier as having "good tonal quality."

Several parallel FEM experiments were done based on Plate #2's model to explore the possible material variations for modification. Based on the prototypes we had, results showed that the main difference between the designs was due to the natural frequency change that accompanied the thickness change of each plate, a finding which may be used as a frequency adjustment measure for future manufacturing.

6.2 Future Work

The vibrational behaviour study of the violin top plate gives us some hints about possible modifications regarding the geometry and the use of new materials to improve or reproduce the violin tonal quality. Similar numerical simulation and experimental tests can also be applied to the back plate, which is usually made of maple. Such work can possibly allow us to study how a composite plate behaves on a whole assembled violin. The results of the plates can form a baseline for the modeling of the whole body of the violin. Some researchers have performed a modal analysis of the violin body; however, the numerical simulation of this process would be far more complex. Since the violin plates are not rigidly glued on the ribs, the boundary conditions would be undoubtedly more difficult to deal with. Also, the air cavity inside the violin body vibrates in a certain pattern. The coupling of the air cavity modes and the body modes would be another challenge.

References

[1] H. Johannsson, "Violin making: Construction." http://aiweb.techfak.uni-bielefeld.de/content/bworld-robot-control-software/. [Online; accessed 04-December-2012].

[2] "Violin student central: The bridge." http://www.violinstudent.com/bridge.html. [Online; accessed 19-January-2013].

[3] P. Avitabile, "Experimental modal analysis," *Sound and vibration*, vol. 35, no. 1, pp. 20–31, 2001.

[4] J. Bretos, C. Santamaria, and J. Moral, "Vibrational patterns and frequency responses of the free plates and box of a violin obtained by finite element analysis," *The Journal of the Acoustical Society of America*, vol. 105, p. 1942, 1999.

[5] N. Molin, L. Lindgren, and E. Jansson, "Parameters of violin plates and their influence on the plate modes," *The Journal of the Acoustical Society of America*, vol. 83, p. 281, 1988.

[6] C. Hutchins, "The acoustics of violin plates," *Scientific American*, vol. 245, no. 4, pp. 170–186, 1981.

[7] J. Moral and C. Hutchins, "From properties of free top plates, of free back plates and of ribs to properties of assembled violins," *Report STL-QPSR*, pp. 1–29, 1984.

[8] C. Hutchins, "A history of violin research," *The Journal of the Acoustical Society of America*, vol. 73, p. 1421, 1983.

[9] C. Hutchins and D. Voskuil, "Mode tuning for the violin maker," *CAS Journal*, vol. 2, no. 4, pp. 5–9, 1993.

[10] N. Molin, M. Tinnsten, U. Wiklund, and E. Jansson, "FEM-analysis of an orthotropic shell to determine material parameters of wood and vibrations modes of violin plates," *Report STL-QPSR*, vol. 4, 1984.

[11] R. Schumacher, "Compliances of wood for violin top plates," *The Journal of the Acoustical Society of America*, vol. 84, p. 1223, 1988.

[12] M. Elejabarrieta, A. Ezcurra, and C. Santamaria, "Vibrational behaviour of the guitar soundboard analysed by the finite element method," *Acta Acustica united with Acustica*, vol. 87, no. 1, pp. 128–136, 2001.

[13] K. Marshall, "Modal analysis of a violin," *The Journal of the Acoustical Society of America*, vol. 77, p. 695, 1985.

[14] E. Jansson and B. Niewczyk, "Experiments with violin plates and different boundary conditions," *The Journal of the Acoustical Society of America*, vol. 86, p. 895, 1989.

[15] G. Bissinger and K. Ye, "Automated hammer-impact modal analysis with a scanning laser vibrometer: working example-a violin," in *SPIE proceedings series*, pp. 943–949, Society of Photo-Optical Instrumentation Engineers, 2000.

[16] D. Oliver, V. Palan, G. Bissinger, and D. Rowe, "3-dimensional laser Doppler vibration analysis of a stradivarius violin," in *Proceedings of the 25th International Modal Analysis Conference, Society for Experimental Mechanics, Bethel, CT, U.S.A.*, 2007.

[17] G. Bissinger and D. Oliver, "3-D laser vibrometry on legendary old italian violins," *Sound and Vibration*, vol. 41, no. 7, pp. 10–15, 2007.

[18] J. Loen, "Reverse graduation in fine cremonese violins," *CAS Journal*, vol. 4, no. 7, pp. 27–39, 2003.

[19] M. Tinnsten and P. Carlsson, "Numerical optimization of violin top plates," *Acta Acustica united with Acustica*, vol. 88, no. 2, pp. 278–285, 2002.

[20] Y. Yu, I. Jang, I. Kim, and B. Kwak, "Nodal line optimization and its application to violin top plate design," *Journal of Sound and Vibration*, vol. 329, no. 22, pp. 4785–4796, 2010.

[21] A. Okuda and T. Ono, "Bracing effect in a guitar top board by vibration experiment and modal analysis," *Acoustical science and technology*, vol. 29, no. 1, pp. 103–105, 2008.

[22] S. Phillips and L. Lessard, "Application of natural fiber composites to musical instrument top plates," *Journal of Composite Materials*, vol. 46, no. 2, pp. 145–154, 2012.

[23] O. Rodgers and T. Masino, "The effect of wood removal on bridge frequencies," *Acoustical Society Journal*, vol. 1, no. 6, pp. 6–10, 1990.

[24] E. Jansson, "Violin frequency response–bridge mobility and bridge feet distance," *Applied Acoustics*, vol. 65, no. 12, pp. 1197–1205, 2004.

[25] G. Bissinger and C. Hutchins, "Tuning the bass bar in a violin plate," *CAS Newsletter*, vol. 26, pp. 10–12, 1976.

[26] L. Condax, "The sound post of the violin," *Catgut Acoust. Soc. Newsletter*, vol. 2, pp. 6–7, 1964.

[27] N. Molin, A. Wåhlin, and E. Jansson, "Transient wave response of the violin body," *The Journal of the Acoustical Society of America*, vol. 88, p. 2479, 1990.

[28] N. Molin, A. Wåhlin, and E. Jansson, "Transient wave response of the violin body revisited," *The Journal of the Acoustical Society of America*, vol. 90, p. 2192, 1991.

[29] G. Knott, "A modal analysis of the violin using MSC/NASTRAN and PATRAN.," tech. rep., DTIC Document, 1987.

[30] P. Mohanty and D. J. Rixen, "Operational modal analysis in the presence of harmonic excitation," *Journal of Sound and Vibration*, vol. 270, no. 1, pp. 93–109, 2004.

[31] M. LeGault, "Acoustical architecture: Making beautiful music," *http://www.compositesworld.com/articles/acoustical-architecture-making-beautiful-music*, 2012.12.02.

[32] O. Rodgers, "Relative influence of plate arching and plate thickness patterns on violin back free plate tuning," *Catgut Acoust. Soc. J.*, vol. 1, p. No.6 (SERIES II), 1990.

[33] I. Curtu, M. Stanciu, C. Itu, and R. Grimberg, "Numerical modeling of the acoustic plates as constituents of stringed instruments," in *Proc. of the 6th International Conference of DAAAM Baltic Industrial Engineering*, pp. 53–58, 2008.

[34] B. Richardson, "Guitar making–the acousticians tale," *Proceedings of the second Vienna talk on music acoustics*, 2010.

[35] M.-N. Lam, "Design and fabrication of a japanese tea table and production of violin tops and tailpieces," tech. rep., McGill University, 2012.

[36] G. Lim, "Optimization of carbon-fiber violin top for maximum loudness," tech. rep., Structures and Composite Materials Laboratory, McGill University, 2010.